



**A physiologically-based pharmacokinetic (PBPK) model of sorafenib  
for investigating the effect of sorafenib parameters  
in hepatorenal impairment**

An internship report in the  
Systems Medicine of the Liver Lab  
Institute for Biology  
Humboldt-Universität zu Berlin

Presented to the  
Faculty of the Clinical Pharmacy/Biochemistry  
Freie Universität Berlin

By Frances Okibedi  
Matric Number: 54233371  
E-Mail: [franceo88@zedat.fu-berlin.de](mailto:franceo88@zedat.fu-berlin.de)

Supervisors  
Dr. Matthias König  
Prof. Charlotte Kloft

January 2024

## Table of content

<b>1 Introduction</b>	<b>5</b>
1.1 Sorafenib	5
1.2 Sorafenib pharmacokinetics	6
1.3 Hepatic and renal impairment	8
1.5 The rationale for the study	9
<b>2 Materials and methods</b>	<b>9</b>
2.1 Data curation	9
2.2 Physiologically-based pharmacokinetic (PBPK) model	10
2.3 Parameter fitting	10
<b>3 Results</b>	<b>13</b>
3.1 Sorafenib database	13
3.2 Physiologically-based pharmacokinetic (PBPK) model for sorafenib	14
3.2.1 Intestinal model	14
3.2.2 Kidney model	15
3.2.3 Liver model	16
3.2.4 Whole-body model	17
3.3 Model application	20
3.3.1 Dose dependency (single & multi dose)	20
3.3.2 Dose-dependent PK parameters	21
3.3.3 Hepatic impairment	21
3.3.4 Renal impairment	23
3.4 Model performance	24
3.4.1 Single oral dose simulation	24
3.4.2 Multiple oral dose simulation	25
3.4.3 Hepatic and renal impairment	26
<b>4 Discussion</b>	<b>27</b>
<b>5 Outlook</b>	<b>30</b>
<b>References</b>	<b>31</b>
<b>Acknowledgements</b>	<b>33</b>

## **Abbreviations**

ABC	ATP Binding Cassette
ABCC2	ATP Binding Cassette C2
ABCC3	ATP Binding Cassette C3
ADME	Absorption, distribution, metabolism and elimination
AUC	Area Under the Curve
BID	Twice a day
CKD	Chronic Kidney Disease
ClCr	Creatinine Clearance
Cmax	Maximum concentration
CTP	Child-Turcotte Pugh
CYP	Cytochrome P450
CYP2C9	Cytochrome P450 2C9
CYP3A4	Cytochrome P450 3A4
GFR	Glomerular Filtration Rate
HCC	Hepatocellular carcinoma
IV	Intravenous
M2	Sorafenib-N-oxide
MRP2	Multidrug Resistance-Associated Protein 2
NAFLD	Non-Alcoholic Fatty Liver Disease
OATP	Organic Anionic Transporter Polypeptide
OATP1B1	Organic Anionic Transport Polypeptide 1B1
OATP2B1	Organic Anionic Transport Polypeptide 2B1
ODE	Ordinary Differential Equation
PBPK	Physiologically based Pharmacokinetic
PO	Oral
RCC	Renal cell carcinoma
SBML	Systems Biology Markup Language
SG	Sorafenib-glucuronide
SNP	Single Nucleotide Polymorphism
UGT1A9	UDP glucuronosyltransferase 1A9

## **Abstract**

Liver cancer ranks second in cancer-related deaths thereby making timely diagnosis and personalized treatment crucial. Hepatocellular carcinoma (HCC) patients often get diagnosed at advanced stages, hindering curative options like resection and ablation. Systemic treatment has become the standard therapy and sorafenib has been the primary systemic treatment for advanced HCC for the last ten years, being the first approved drug for this purpose. Sorafenib (Nexavar), is a multi-kinase inhibitor medication approved for primarily treating advanced renal cell carcinoma, hepatocellular carcinoma or other cancers.

After oral administration, sorafenib enters hepatocytes via OATP1B-type carriers. It undergoes CYP3A4-mediated oxidative metabolism to sorafenib-N-oxide (M2) and UGT1A9-mediated glucuronidation forming sorafenib-glucuronide (SG). SG is secreted into bile mainly by ABCC2, with a fraction reuptaken by ABCC3, preventing ABCC2 saturation. In bile, SG can be excreted via the feces or converted back to sorafenib by a bacterial  $\beta$ -glucuronidase. Sorafenib is absorbed in the intestine, reentering the systemic circulation, contributing to elimination and detoxification. Sorafenib is excreted mainly by the feces (77%) and urine (19%). Hepatic and renal impairment could have a large impact on the pharmacokinetics of sorafenib.

Within this work the pharmacokinetics of sorafenib were analyzed by developing a physiologically-based pharmacokinetic (PBPK) model based on extensive data curation of sorafenib data. The model allowed to simulate the time-concentration courses of sorafenib in various tissues and to calculate the pharmacokinetic parameters for sorafenib under single and multiple dosing regimes. The model was applied to study the dose-dependency of sorafenib treatment and to investigate the effect of hepatic and renal impairment on sorafenib pharmacokinetics.

# 1 Introduction

## 1.1 Sorafenib

Sorafenib (NEXAVAR®, BAY43-9006) is a FDA-approved oral anti-cancer medication for advanced renal cell carcinoma (RCC), unresectable or metastatic hepatocellular carcinoma (HCC), and locally recurrent or metastatic, progressive differentiated thyroid carcinoma (DTC) refractory to radioactive iodine treatment [1]. It is also under evaluation for acute myeloid leukemia (AML) and other solid tumors in both adults and children. Sorafenib hinders tumor cell proliferation and angiogenesis by targeting various serine/threonine and tyrosine kinases (RAF1, BRAF, VEGFR1, VEGFR2, VEGFR3, PDGFR, KIT, FLT3, FGFR1, RET) in multiple oncogenic signaling pathways [1].

**Mechanism of Action:** Sorafenib functions as a multi-protein kinase inhibitor, targeting various protein kinases such as VEGFR, PDGFR, and RAF kinases. Notably, it exhibits greater selectivity for c-Raf over B-RAF among RAF kinases. The drug induces autophagy during treatment, potentially inhibiting tumor growth. Additionally, due to its 1,3-disubstituted urea structure, sorafenib serves as a potent soluble epoxide hydrolase inhibitor, likely mitigating the severity of its adverse effects [1].

## 1.2 Sorafenib pharmacokinetics

The pharmacokinetics (PK) of a drug describes the changes of the drug concentration in the body after its administration due to absorption, distribution, metabolism and elimination (ADME) [2]. An overview of the processes involved in sorafenib's PK is described below and depicted in Figure 1.

**Absorption:** Sorafenib is a small, lipophilic molecule characterized by low solubility and high permeability. Following oral administration, it undergoes rapid absorption from the gastrointestinal tract, reaching the liver via the portal vein. Peak plasma levels are attained within 1 to 12 hours, with a longer duration observed in the fed state. Steady-state concentrations are typically achieved around the seventh day. Sorafenib exhibits a mean half-life ranging from approximately 20 to 48 hours at a dose of 400 mg twice a day (bid) [2].

**Metabolism:** After oral absorption sorafenib undergoes primary metabolism in the liver through two main pathways: phase I oxidation, mediated by cytochrome P450 3A4 (CYP3A4) to form to sorafenib-N-oxide (M2), and phase II conjugation, mediated by UDP glucuronosyltransferase 1A9 (UGT1A9) to form sorafenib-glucuronide (SG). After conjugation, SG is extensively secreted into the bile via ABCC2. In bile, SG can be excreted or converted back to sorafenib by a bacterial  $\beta$ -glucuronidase. Sorafenib is absorbed in the intestine, reentering the systemic circulation, contributing to elimination and detoxification. Eight metabolites of sorafenib have been identified, labeled as M1-M8. M2 is the predominant metabolite in the plasma constituting 9 – 16% of the circulating analytes under steady-state conditions and exhibits comparable potency to sorafenib in-vitro [2].

M2 is further transformed into N-hydroxymethyl-sorafenib-N-oxide (M1) and glucuronidated to form M8. The M7 is (SG). Glucuronidation is responsible for approximately 15% of sorafenib clearance in humans, whereas oxidation accounts for only 5%. The M2, M4 (demethylation), and M5 (oxidative metabolite) have been identified as inhibitors of the Vascular Endothelial Growth Factor Receptor (VEGFR) signaling pathway, Platelet-Derived Growth Factor Receptor (PDGFR) signaling pathway, and members of the Mitogen-Activated Protein Kinase (MAPK) pathway [2].

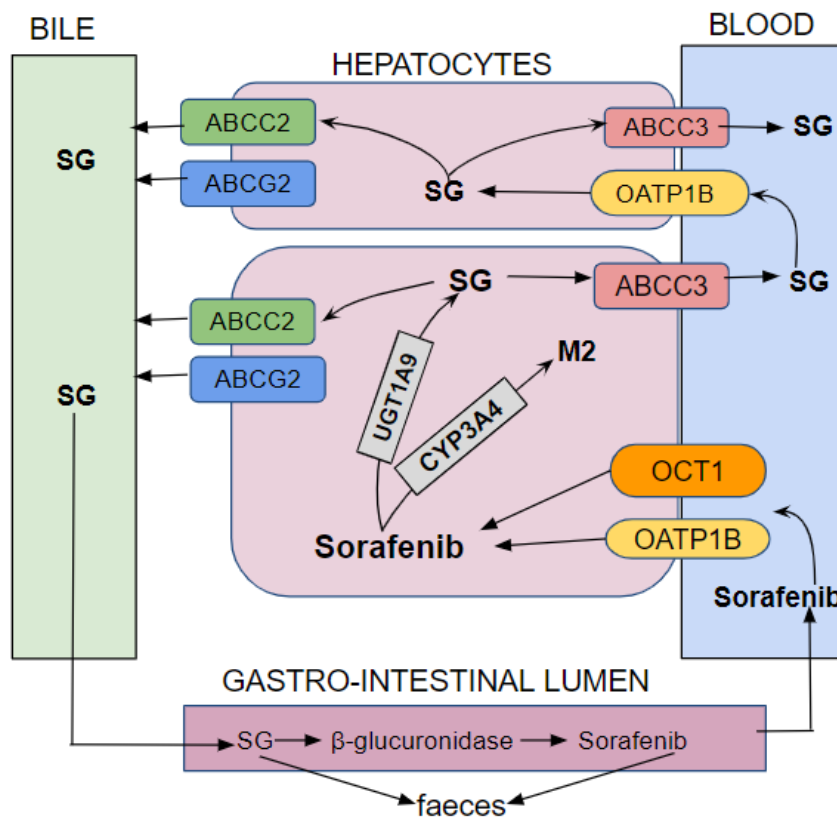


**Figure 1: Overview of sorafenib metabolism and pharmacokinetics in humans.** After oral administration, sorafenib enters hepatocytes via transport mechanisms which includes OATP1B-type carriers and OCT1. Subsequently, sorafenib undergoes CYP3A4-mediated metabolism to sorafenib-N-oxide (M2), and UGT1A9-mediated glucuronidation to form sorafenib-glucuronide (SG). After conjugation, SG is secreted into bile mainly by ABCC2 and partly by ABCG2. From the bile SG can be excreted due to enterohepatic circulation via the feces or converted back to sorafenib by a bacterial  $\beta$ -glucuronidase. Sorafenib is absorbed in the intestine, reenters the systemic circulation, contributing to elimination and detoxification [2].

**Excretion:** The majority (77%) of the drug is excreted in the feces, with 51% remaining unchanged, while approximately 19% is eliminated in the urine, primarily as glucuronide conjugates of the parent drug and its metabolites [2].

**Toxicity and safety:** The most frequently observed negative effects linked to sorafenib encompass hand-foot skin reaction (HFSR), diarrhea, hypertension, rash, fatigue, abdominal pain, and nausea. Although severe adverse effects such as liver failure and myocardial infarction are uncommon, they may occur in certain instances [2].

Adverse events have the potential to impact treatment efficacy by necessitating dose reduction or treatment interruptions. Cumulative drug exposure and responses to sorafenib treatment exhibit considerable variability among individual patients [2].

**Pharmacokinetic parameters:** Multiple dosing of sorafenib revealed significant interpatient pharmacokinetic variability. Clinical trials demonstrated variations in sorafenib exposure (area under the plasma drug concentration-time curve (AUC)) ranging from 18.0 to 24.0 mg·h/l on day 1 and 47.8 to 76.5 mg·h/l on the last day of the dosing cycle. Peak plasma concentrations (Cmax) showed a range of 2.3 to 3.0 mg/l on day 1 and 5.4 to 10.0 mg/l on the last day of dosing [2]. The median time to peak plasma concentration (Tmax) varied from 2 to 12 hours. Moreover, sorafenib's AUC and Cmax values exhibited less than proportional increases with higher doses [2]. The incidence and severity of sorafenib-induced side effects, such as hand-foot skin reaction (HFSR), were linked to cumulative dose and sorafenib exposure level [2]. The underlying mechanisms for these variabilities remain incompletely understood, and no validated markers have been identified to predict clinical outcomes or tolerability for sorafenib [2].

### 1.3 Hepatic and renal impairment

The liver and kidneys play crucial roles in eliminating sorafenib. Impairment in hepatic or renal function can have a substantial impact on sorafenib pharmacokinetics, particularly in patients treated for hepatocellular carcinoma (HCC) or renal cell carcinoma (RCC) who often have compromised liver function. This is also relevant for older patients with impaired renal function. Understanding these effects is crucial for optimizing dosage and improving therapy outcomes.

**Hepatic impairment:** This refers to inadequate liver function resulting from conditions like liver injury or diseases such as cirrhosis, often caused by chronic hepatitis C virus infection or Non-Alcoholic Fatty Liver Disease (NAFLD). Cirrhosis involves liver tissue degeneration, hepatocyte necrosis, and scarring, leading to distorted hepatic vasculature which affects blood supply, causing portal hypertension and potentially forming hepatic shunts that bypass parts of the liver. The severity of cirrhosis can be assessed using the Child-Turcotte Pugh (CTP) scoring system, with Class A indicating good function, Class B moderate function, and Class C severe dysfunction. Understanding the impact of cirrhosis on sorafenib's pharmacokinetics is crucial, as it can affect drug clearance, plasma protein binding, and distribution mechanisms [1].

**Renal impairment:** Chronic Kidney Disease (CKD) leads to progressive renal function failure, which can be quantified through the Glomerular Filtration Rate (GFR), e.g. by using creatinine Clearance (ClCr) for estimation of the GFR. Normal GFR is 90 ml/min/1.73m<sup>2</sup> or higher, decreasing significantly in patients with kidney failure (i.e. eGFR is <60 mL/min/1.73m<sup>2</sup> for over three months in CKD). Lower renal function correlated with reduced sorafenib clearance. Studies indicate that when eGFR falls below <45 mL/min/1.73m<sup>2</sup>, there is a rapid increase in all-cause mortality, cardiovascular events, and hospitalization rates [6]. Cancer patients taking sorafenib often suffer from hepatic and renal impairment, e.g. due to hepatocellular or renal cancer. These patients are often of advanced age which is associated with declining renal and liver function [1].

#### **1.4 Physiologically-based pharmacokinetic (PBPK) model**

Physiologically-based pharmacokinetic (PBPK) models allow the investigation of the PK of a specific substance through computational modeling [1]. These models facilitate the prediction of the ADME's (absorption, distribution, metabolism and excretion) processes within the human body. These models are based on systems of Ordinary Differential Equations (ODEs) which simulate the time-dependency of processes and metabolites in various compartments. PBPK models consist of distinct compartments representing different organs or tissues, interconnected through blood flow. These models prove valuable in comprehending the impact of alterations in components and processes, such as different haplotypes in transporters or alterations in different pathophysiologies such as hepato-renal impairment. PBPK models are particularly advantageous for examining how physiological changes or disease-related modifications affect drug pharmacokinetics, such as in cases of varying degrees of cirrhosis or renal impairment [2].

#### **1.5 The rationale for the study**

Liver cancer is the second most common cause of cancer-related death. Diagnosis and treatment are time-critical and require highly patient-specific diagnostic and treatment pathways. Medical decision-making is based on a variety of interdependent factors related to different medical disciplines, past experience and clinical guidelines. Most patients with hepatocellular carcinoma (HCC) are diagnosed at an advanced stage of the disease, which precludes curative therapy such as resection and ablation, making systemic treatment the standard of care. Although improvements in surveillance programmes allow for early diagnosis and curative treatment, nearly half of all patients with HCC ultimately receive systemic therapy. Sorafenib was the first systemic drug approved for the treatment of HCC and has been the first-line option for advanced HCC for the past decade. Currently, there is no open dataset of curated pharmacokinetic data for the protein kinase inhibitor sorafenib, despite its use in first-line treatment of various cancers. For example, sorafenib is not only approved for the first-line treatment of HCC, but also for the treatment of renal cell carcinoma and advanced thyroid cancer. This project established a high-quality database for sorafenib PKs in liver cancer therapy. The PK data was used to create a PBPK model for systemic sorafenib therapy in liver cancer to answer key questions about sorafenib suitability in advanced liver cirrhosis, such as dose dependency of pharmacokinetics and effect of hepatic and renal impairment on sorafenib pharmacokinetics.

#### **Objectives of the study**

The specific objectives of the internship were:

- Establish a PK database of sorafenib for model building and validation
- Develop a computational model of sorafenib (physiological based whole-body model, ordinary differential equations) for adults
- Investigate the effect of dose dependency on sorafenib pharmacokinetics
- Investigate the effect of hepatic and renal impairment on sorafenib pharmacokinetics

## 2 Materials and methods

The development of the sorafenib PBPK model consisted of curation of literature data for model calibration and validation, followed by model development and simulation, then parameter optimization, and calculation of PK parameters from time-course data and simulations.

### 2.1 Data curation

The sorafenib data curation process included an extensive literature search for sorafenib PK studies, digitization and storage of relevant literature data. Literature searches were performed using PKDPAI (<https://www.pkdai.com/>) and PubMed (<https://pubmed.ncbi.nlm.nih.gov/>) using various queries such as “sorafenib AND pharmacokinetics” to identify relevant publications. The literature management tool zotero (<https://www.zotero.org/>) was used to screen, filter and prioritize the search results based on the presence of data related to sorafenib pharmacokinetics from healthy subjects, and patients with renal and hepatic functional impairment. The selected studies were reviewed to extract relevant data such as subject characteristics, group demographics (including age, sex, body weight, health status, ethnicity, body surface area), sorafenib dosing protocol, PK parameters and PK time courses. Data was digitized using PlotDigitizer (<https://sourceforge.net/projects/plotdigitizer/>) from figures, tables and textual descriptions in the 16 selected sorafenib studies. All information was stored in a standardized format based on Microsoft Excel using established data curation protocols for pharmacokinetic information [3]. The dataset was reviewed by Dr. Matthias König, and was uploaded to the open source PK database (PK-DB, <https://pk-db.com>) [3].

### 2.2 Physiologically-based pharmacokinetic (PBPK) model

The sorafenib PBPK model was created in Python using the Systems Biology Markup Language (SBML, <https://sbml.org/software/>) [4], [5] with model development and visualization being performed with sbmlutils [6] and cy3sbml [7], [8]. The model consists of a system of ordinary differential equations (ODEs) solved numerically using sbmlsim [9], which is based on the high-performance SBML simulator libroadrunner [10], [11]. The developed sorafenib PBPK model follows a hierarchical structure, consisting of a whole-body model that connects different sub-models for organs such as intestine, kidney and liver via the systemic circulation. The biochemical reactions within the model describe the import and export of sorafenib between the plasma and organs and metabolic conversions. The intestinal import mediated by OATP2B1 was modeled by irreversible first-order Michaelis-Menten kinetics, while the sorafenib export reaction followed irreversible mass-action kinetics. Hepatic impairment was modeled as previously described by Köller et al., [12], [13]. Renal impairment was modeled as a stepwise decrease in renal function by scaling all renal processes with the factor f\_renal\_function, where 1.0 represents normal function and 0.0 represents no renal function as described by Stemmer et al. 2023 [14].

Individual intestine, liver and kidney models, as well as the whole-body model, are available in SBML format from the following repository: <https://github.com/matthiaskoenig/sorafenib-model>. Within this work v0.9.1 of the model was used [15].

### 2.3 Parameter fitting

Parameter fitting is an optimization method for adjusting model parameters  $\vec{p} = (p_1, \dots, p_n)$  in order to minimize the difference between model predictions and experimental data. The fitting process involves minimizing the residuals (denoted as  $r$ ) between model predictions  $f(x_{i,k})$  and experimental data  $y_{i,k}$  using an objective cost function ( $F$ ).

The SciPy least-squares method was used as the cost function ( $F$ ), depending on the parameters  $\vec{p}$  and following an L2-norm corresponding to the sum of the weighted residuals as described by:

$$F(\vec{p}) = \frac{1}{2} \sum_{i,k} (w_k \cdot w_{i,k} r_{i,k})^2$$

where:

$w_k$  describes the weighting factor of time course k,

$w_{i,k}$  describes the weighting of the respective data point i of time course k based on the error of the data point, and

$r_{i,k} = (y_{i,k} - f(X_{i,k}))$  represents the residual of time i of time course k.

### 2.4 Sorafenib pharmacokinetic parameters

The following formulas were used for calculation of pharmacokinetic parameters from the plasma concentration time courses.

**Maximum concentration,  $c_{max}$  [ $\mu M$ ]:** This is the peak sorafenib plasma concentration. It is calculated by finding the maximal concentration value in the time-course.

**Elimination rate,  $k_{el}$  [1/min]:** This is a measure for the elimination of a substance. The elimination rate is calculated assuming an exponential decrease of a substance by the equation:

$$sor(t) = sor(0) \cdot e^{-k_{el} \cdot t}$$

A linear regression is performed in logarithmic space to calculate  $k_{el}$ .

**Area Under the Curve, AUC [ $\text{mg}\cdot\text{hr}/\text{ml}$ ]:** This describes the area under the concentration time curve. This parameter can be calculated via the trapezoidal rule:

$$AUC_{0 \rightarrow tn} = \frac{1}{2} \sum_{i=1}^{n-1} (t_{i+1} - t_i) \cdot (C_{i+1} + C_i)$$

The AUC between the last measured time point  $t_{last}$  and infinity can be calculated by the

$$\text{equation: } AUC_{last \rightarrow \infty} = \frac{C_{last}}{K_{el}}$$

$AUC_{0 \rightarrow \infty}$  describes the AUC extrapolated to infinity calculated as:

$$AUC_{0 \rightarrow \infty} = AUC_{0 \rightarrow last} + AUCl_{last \rightarrow \infty}$$

**Volume of distribution,  $V_d$  [l]:**  $V_d$ s is a virtual compartment which describes the tendency of a drug to either circulate in plasma or to disperse to other tissue compartments. This parameter can be calculated by the following equation:  $V_d = AUC \cdot k_{el}$

**Clearance,  $Cl$  [ml/min]:** The clearance describes the ability of the body to excrete a drug. This parameter is calculated by multiplying the rate of elimination  $k_{el}$  with the volume of distribution  $V_d$ , as described by equation:  $Cl = k_{el} \cdot V_d$

**Half life,  $t_{half}$  [min]:** The half life is defined by the time required for serum or plasma concentration of sorafenib to be reduced by 50%. This parameter can be calculated from the rate of elimination  $k_{el}$  via:  $t_{half} = \frac{\ln(2)}{k_{el}}$

**Bioavailability,  $F$  [%]:** The bioavailability refers to the fraction of a drug which reaches the systemic circulation when comparing an oral dose with an intravenous dose. The bioavailability can be calculated from the AUC of an oral and a respective intravenous dose via equation below:

$$F = \frac{AUC_{po}}{AUC_{iv}} \cdot \frac{dose_{iv}}{dose_{po}}$$

Where po is the oral application and iv is the intravenous application.

**Renal clearance  $Cl_{Renal}$  [l/min]:** This describes the clearance of a drug by the kidneys. This renal clearance can be calculated by dividing the amount of sorafenib recovered in urine over a given time by the AUC in plasma over the same period:

$$Cl_{Renal} = \frac{AR_{\Delta t}}{AUC_{\Delta t}}$$

Where AR is the amount of sorafenib recovered in urine from time 0 to time  $\Delta t$  hours [10].

**Hepatic clearance,  $Cl_{Hepatic}$  [l/min]:** This describes the clearance of a drug by the liver. The hepatic clearance is calculated by subtracting the renal clearance from the total clearance (assuming only kidneys and liver are involved in the clearance):

$$Cl_{Hepatic} = Cl_{total} - Cl_{renal}$$

## 3 Results

### 3.1 Sorafenib database

A systematic literature research for sorafenib pharmacokinetics information was performed. Based on the results a sorafenib database consisting of 16 publications on sorafenib treatment in patients with HCC, RCC and other cancers has been curated (Tab. 1). The data is available via the PK-DB database <https://pk-db.com/>.

**Table 1: Overview of the sixteen curated literature data.**

Reference	PK-DB ID	PMID	Dose (mg)	Health status	Study description
Aboualfa2006 [16]	<a href="#">PKDB00721</a>	<a href="#">16908937</a>	200	HCC	Phase II study of sorafenib in patients with advanced hepatocellular carcinoma.
Andriamanana2013 [17]	<a href="#">PKDB00722</a>	<a href="#">23562906</a>	400 bid	HCC	Simultaneous analysis of anticancer agents bortezomib, imatinib, nilotinib, dasatinib, erlotinib, lapatinib, sorafenib, sunitinib and vandetanib in human plasma using LC/MS/MS
Awada2005 [18]	<a href="#">PKDB00723</a>	<a href="#">15870716</a>	100, 200, 300, 400, 600, 800 QD	HCC	Phase I safety and pharmacokinetics of BAY 43-9006 administered for 21 days on/7 days off in patients with advanced, refractory solid tumours.
Bins2017 [19]	<a href="#">PKDB00724</a>	<a href="#">28371445</a>	200, 400 bid	HCC	Influence of OATP1B1 function on the disposition of Sorafenib-β-D-Glucuronide.
Duran2007 [20]	<a href="#">PKDB00725</a>	<a href="#">17699864</a>	200, 400 bid	HCC RCC	Phase I targeted combination trial of sorafenib and erlotinib in patients with advanced solid tumors
Ferrario2016 [21]	<a href="#">PKDB00726</a>	<a href="#">27992451</a>	200 bid	Breast cancer	Phase I/II trial of sorafenib in combination with vinorelbine as first-line chemotherapy for metastatic breast cancer.
Fucile2015 [22]	<a href="#">PKDB00727</a>	<a href="#">25429830</a>	200 400 bid	HCC	Measurement of sorafenib plasma concentration by high-performance liquid chromatography in patients with advanced hepatocellular carcinoma: is it useful in clinical practice? A pilot study
Fukudo2014 [23]	<a href="#">PKDB00728</a>	<a href="#">24135988</a>	400 bid	HCC RCC	Exposure-toxicity relationship of sorafenib in Japanese patients with renal cell carcinoma and hepatocellular carcinoma.
Hornecker2012 [24]	<a href="#">PKDB00729</a>	<a href="#">22006162</a>	200, 800, 1200, 1600, 2000, 2400 QD	HCC, RCC Thyroid cancer	Saturable absorption of sorafenib in patients with solid tumors: a population model.
Huang 2017 [25]	<a href="#">PKDB00730</a>	<a href="#">28741453</a>	200 400 QD	thyroid cancer	No effect of levothyroxine and levothyroxine-induced subclinical thyrotoxicosis on the pharmacokinetics of sorafenib in healthy male subjects.
Hub2021 [26]	<a href="#">PKDB00731</a>	<a href="#">33925058</a>	100, 150 200 QD	healthy	Population pharmacokinetic modeling and simulation to determine the optimal dose of nanoparticulated sorafenib to the reference sorafenib.
Hussaarts2020 [27]	<a href="#">PKDB00732</a>	<a href="#">12090788</a>	200, 400 600, 800	HCC Thyroid cancer	Influence of probenecid on the pharmacokinetics and pharmacodynamics of sorafenib
Ishii2014 [28]	<a href="#">PKDB00733</a>	<a href="#">23639221</a>	200 QD	HCC	Sorafenib in a hepatocellular carcinoma patient with end-stage renal failure: A pharmacokinetic study.
Mammatas2020 [29]	<a href="#">PKDB00734</a>	<a href="#">32274565</a>	1000, 2000 2400, 2800 QD	HCC, RCC, bile, pancreas, uterus, breast cancer etc	Sorafenib administered using a high-dose, pulsatile regimen in patients with advanced solid malignancies: a phase I exposure escalation study.
Strumberg2005 [30]	<a href="#">PKDB00735</a>	<a href="#">15613696</a>	100, 200, 400, 600, 800 bid	HCC, RCC, breast, colon, pancreas, skin, GI cancer	Phase I clinical and pharmacokinetic study of the novel Raf kinase and vascular endothelial growth factor receptor inhibitor BAY 43-9006 in patients with advanced refractory solid tumors.
Zimmerman2012 [31]	<a href="#">PKDB00736</a>	<a href="#">22927483</a>	150, 200 bid	acute leukemia	Ontogeny and sorafenib metabolism

### **3.2 Physiologically-based pharmacokinetic (PBPK) model for sorafenib**

Based on the established database, a sorafenib PBPK model was developed to investigate its PK characteristics and to simulate its time-courses in plasma and tissues (liver, bile, kidney). The model consists of tissue models for the intestine, kidney, and liver, which were coupled to the systemic circulation to generate a whole-body model.

#### **3.2.1 Intestinal model**

The intestinal model describes the absorption of sorafenib after oral administration (Fig. 3.1). Sorafenib is absorbed in the upper small intestine by OATP2B1 into the blood. The unabsorbed remainder is excreted into feces. The fraction absorbed is determined by the parameter F\_sor\_abs. The irreversible uptake of OATP2B1 is modeled using Michaelis-Menten kinetics:

$$absorption = \frac{SORABS_{V_{max}} \cdot V_{gu} \cdot [sor\_lumen]}{([sor\_lumen] + SORABS_{Km})}$$

SORABS\_Vmax represents the maximum absorption velocity of sorafenib into the liver, with Vgu being the volume compartment in the intestine. [sor\_lumen] denotes sorafenib concentration in the intestinal lumen, and SORABS\_Km indicates the enzyme-substrate affinity between sorafenib and OATP2B1.

The fraction excreted into feces was defined as:

$$excretion_{sor} = (1 - F_{sor\_abs}) \cdot absorption$$

Sorafenib N-Oxide glucuronide (SG) can also be absorbed or excreted in the intestine to describe enterohepatic circulation of the substance.

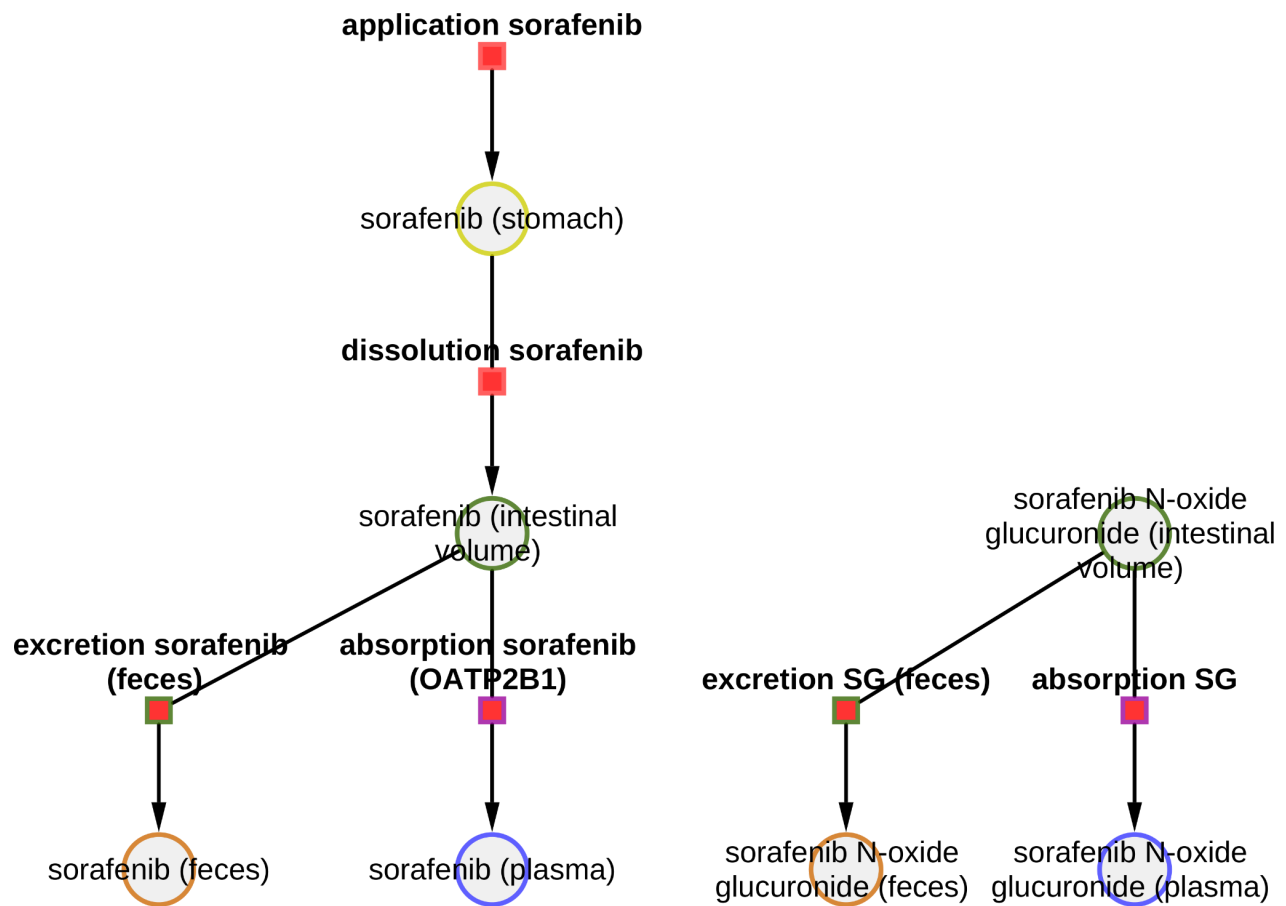


**Figure 3.1: Overview of sorafenib intestine model.** Depicted are the absorption of sorafenib (SOR) in the intestine, transport of sorafenib via OATP2B1 into the plasma and excretion through feaces as well as absorption of sorafenib-glucuronide (SG) into plasma and excretion of SG via feaces.

### 3.2.2 Kidney model

The kidney model (Fig. 3.2) describes the renal elimination of sorafenib glucuronide in urine by the kidneys using mass-action kinetics.

$$\text{excretion} = f_{\text{renal\_function}} \cdot SGEX_k \cdot Vki \cdot [sg_{\text{ext}}]$$

Neither sorafenib nor sorafenib N-oxide are excreted by the kidneys.

The parameter  $f_{\text{renal\_function}}$  was varied from 0.1 to 1.9 to systematically assess the effects of changes in renal function with a value of 1.0 for normal kidney function, less than 1.0 for reduced function, and greater than 1.0 for increased function.  $SGEX_k$  is the rate constant describing the urinary excretion rate of sorafenib.  $Vki$  is the kidney volume and  $[sg_{\text{ext}}]$  is the sorafenib N-Oxide glucuronide (SG) concentration in the plasma of the kidneys.

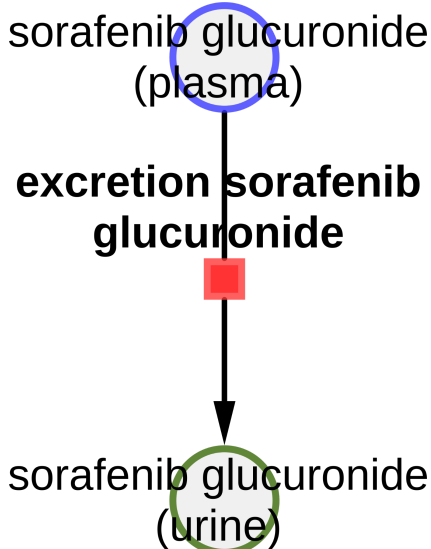


**Figure 3.2: Overview of sorafenib kidney model.** Sorafenib-glucuronide (SG) can be excreted via the kidneys from the plasma.

### 3.2.3 Livermodel

The liver model (Fig 3.3) describes the hepatic uptake of sorafenib (SOR) via OAPT1B/OCT1 into the liver, sorafenib oxidation by CYP3A4 to sorafenib-N-oxide (M2), and M2 glucuronidation via UGT1A9 to sorafenib-glucuronide (SG) which is excreted into the bile via ABCC2/ABCG2. After entering the bile, sorafenib undergoes enterohepatic circulation, re-entering the intestinal lumen for potential reabsorption or fecal excretion. The import of sorafenib into the liver is defined by:

$$import_{sor} = \frac{SORIM_{V_{max}} \cdot Vli \cdot [sor\_ext]}{([sor\_ext] + SORIM_{Km\_sor})}$$

$Vli$  is the liver volume, and  $[sor\_ext]$  is the sorafenib concentration in hepatic plasma.  $SORIM_{Km\_sor}$  and  $SORIM_{Vmax}$  represent the affinity of OATP1B1 for sorafenib and the maximal velocity, respectively. The export of sorafenib into the liver is defined by:

$$export_{sor} = \frac{SOREX_{Vmax} \cdot Vli \cdot [sor]}{([sor] + SOREX_{Km\_sor})}$$

The export of sorafenib into the bile is determined by  $Vli$  (liver volume) and  $[sor]$  (sorafenib concentration in the liver).  $SOREX_{Km\_sor}$  and  $SOREX_{Vmax}$  denote the affinity of for sorafenib and the maximal velocity, respectively.

The enterohepatic circulation (EHC<sub>sg</sub>) is modeled by an irreversible transport of sorafenib glucuronide from the liver in the bile with subsequent EHC from bile to the intestinal lumen:

$$EHC_{sg} = SGEHC_k \cdot Vli \cdot sg\_bi$$

where  $Vli$  is the liver volume,  $SGEHC_k$  is the rate of sorafenib glucuronide transport in the enterohepatic circulation, and  $sg\_bi$  is the amount in the bile.

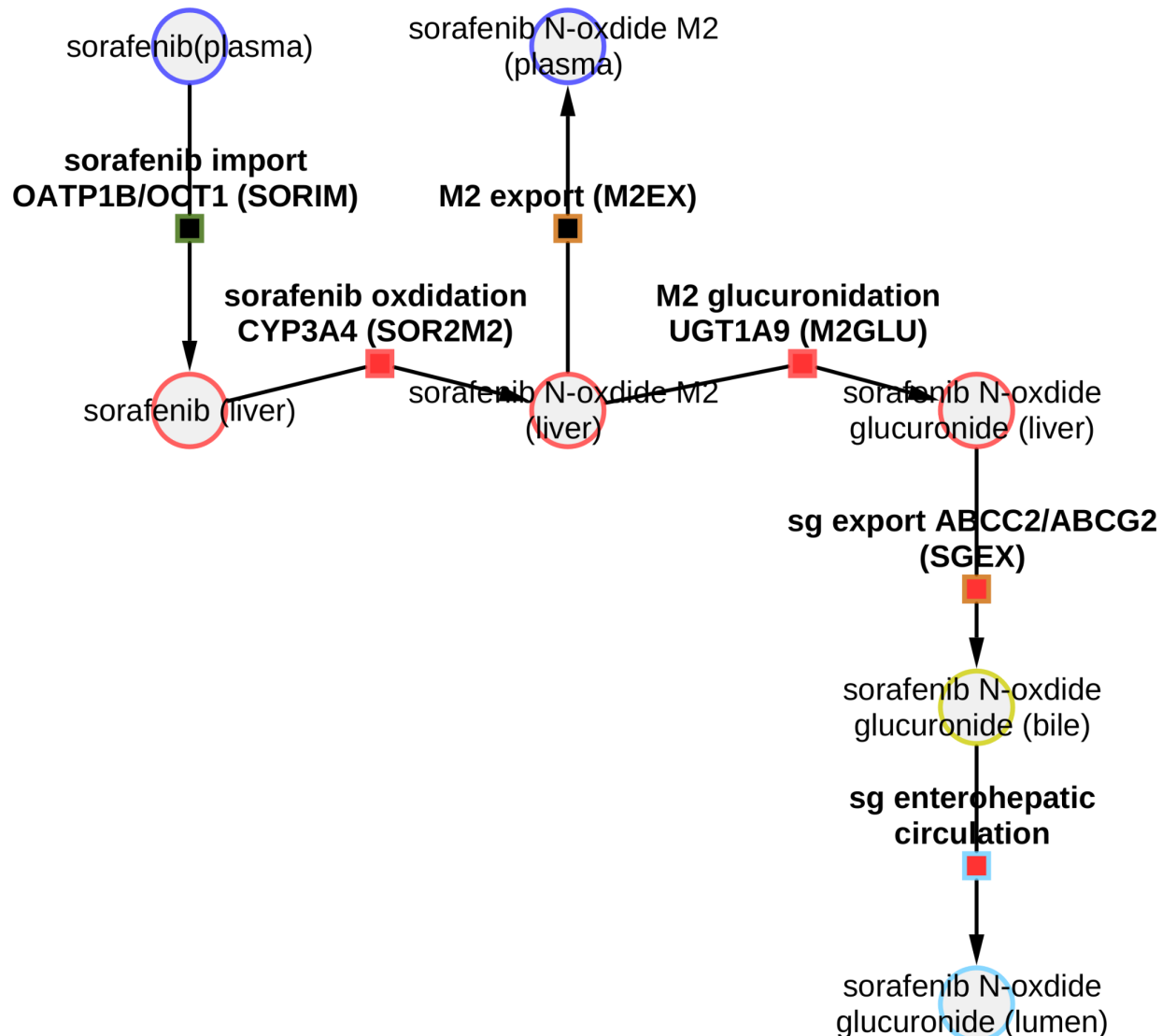


**Figure 3.3: An overview of sorafenib liver model.** Depicting the transport of sorafenib (SOR) via OAPT1B/OCT1 into the liver, sorafenib oxidation by CYP3A4 to sorafenib-N-oxide (M2), M2 glucuronidation via UGT1A9to sorafenib-glucuronide (SG) which is excreted to the bile by ABCC2/ABCG2 transporter then SG undergoes enterohepatic circulation (EHC) by reabsorption into the lumen.

### 3.2.4 Whole-body model

The whole body mody integrates the tissue models of the intestine, liver, and kidney to simulate the distribution of sorafenib, M2 and SG through the systemic circulation (Fig 3.4). The metabolites are transported via blood to the various tissues, and the enterohepatic circulation allows SG to reach the intestine from the liver via bile.

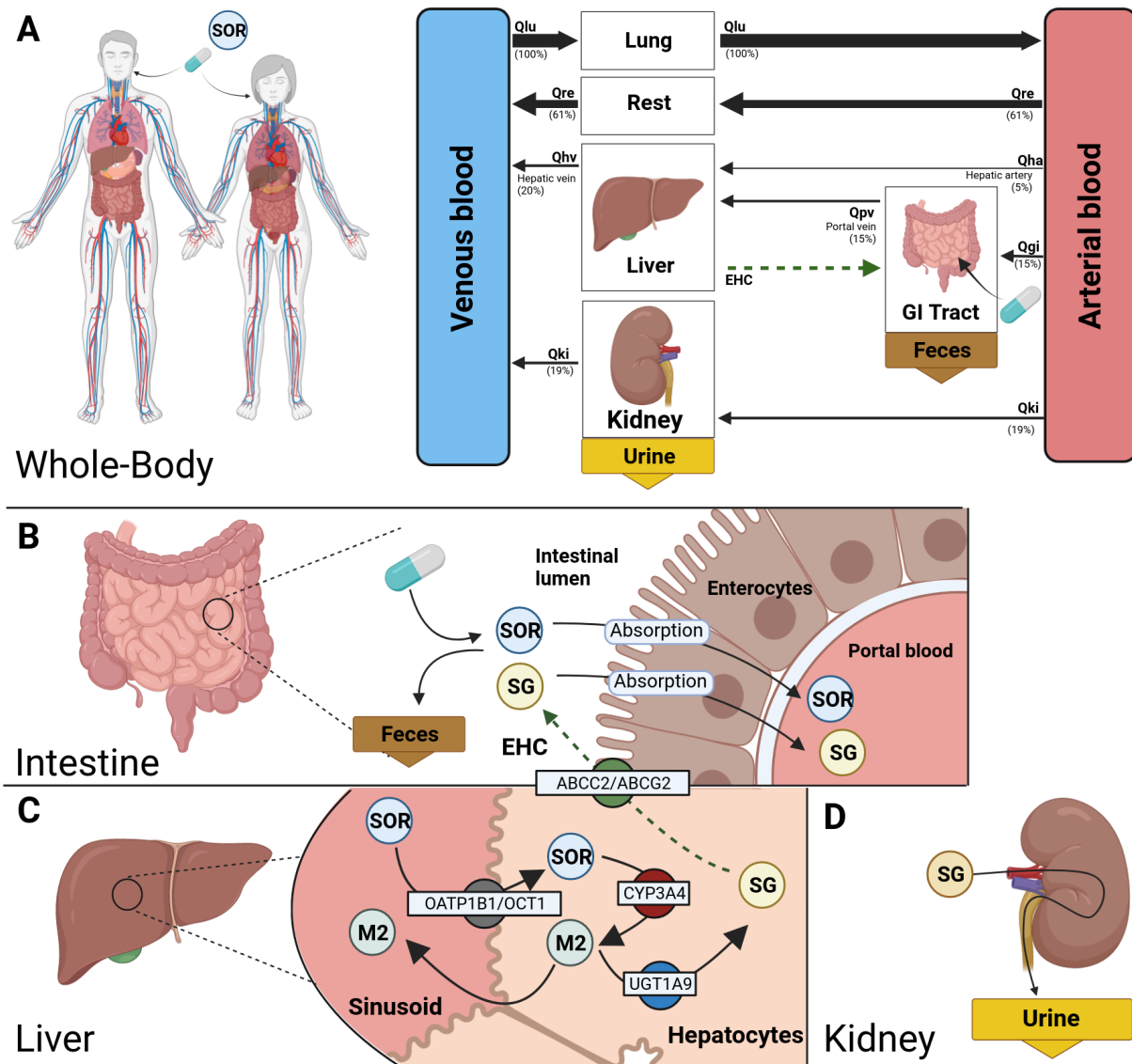


**Figure 3.4 Physiologically-based pharmacokinetic (PBPK) model of sorafenib depicting the intestinal, liver and kidney model. (A)** The whole-body model illustrates the oral administration of sorafenib and connection of tissues and compartments through venous and arterial blood flow, enabling sorafenib distribution in the body, particularly its target site, the liver. **(B)** The intestinal model consists of the dissolution, absorption of sorafenib (SOR) from the intestinal lumen into the blood and fecal excretion and enterohepatic circulation of sorafenib-glucuronide (SG). **(C)** The liver model consists of uptake of sorafenib from the blood into hepatocytes via OATP1B1/OCT1 where sorafenib is metabolized by oxidation via CYP3A4 to sorafenib-N-oxide (M2) and by conjugation via UGTP19 to sorafenib glucuronide (SG). SG is subsequently excreted into the bile via ABCC2/ABCG2 shown as the dashed arrow. SG is transported from the bile into the intestine via the enterohepatic circulation (EHC) **(D)** The kidney model consists of urinary excretion of sorafenib-glucuronide (SG). Created with Biorender.

### 3.2.5 Model of cirrhosis and renal functional impairment

**Hepatic functional impairment (cirrhosis):** Liver cirrhosis entails both intrahepatic shunts of the total liver blood supply and hepatic tissue loss. Due to these physiological changes, a fraction of sorafenib cannot reach the liver and the liver has a reduced effective volume for the metabolism of sorafenib.

The cirrhosis model established by Köller et al. [1, 2] was used (Fig. 3.5A). The parameter  $f_{\text{shunts}}$  describes the fraction of blood shunted around the liver, ranging from 0.0 (no shunting) to 0.9 (90% shunting). The remaining blood reaching the liver is defined as  $1 - f_{\text{shunts}}$ .  $F_{\text{tissue\_loss}}$  represents the loss of functional tissue volume, ranging from 0.0 (no tissue loss) to 0.9 (90% tissue loss). The parameter  $f_{\text{cirrhosis}}$  combines  $f_{\text{shunts}}$  and  $F_{\text{tissue\_loss}}$ , varying from 0.0 to 0.9. A value of 0.0 signifies a healthy liver, while 0.9 indicates severe cirrhosis. Modifying  $f_{\text{cirrhosis}}$  allows the reproduction of different degrees of hepatic functional impairment. The values for  $f_{\text{cirrhosis}}$  used in the study was 0 for the control group, 0.40 for mild cirrhosis (CPT-A), 0.70 for moderate cirrhosis (CPT-B), 0.81 for severe cirrhosis (CPT-C).

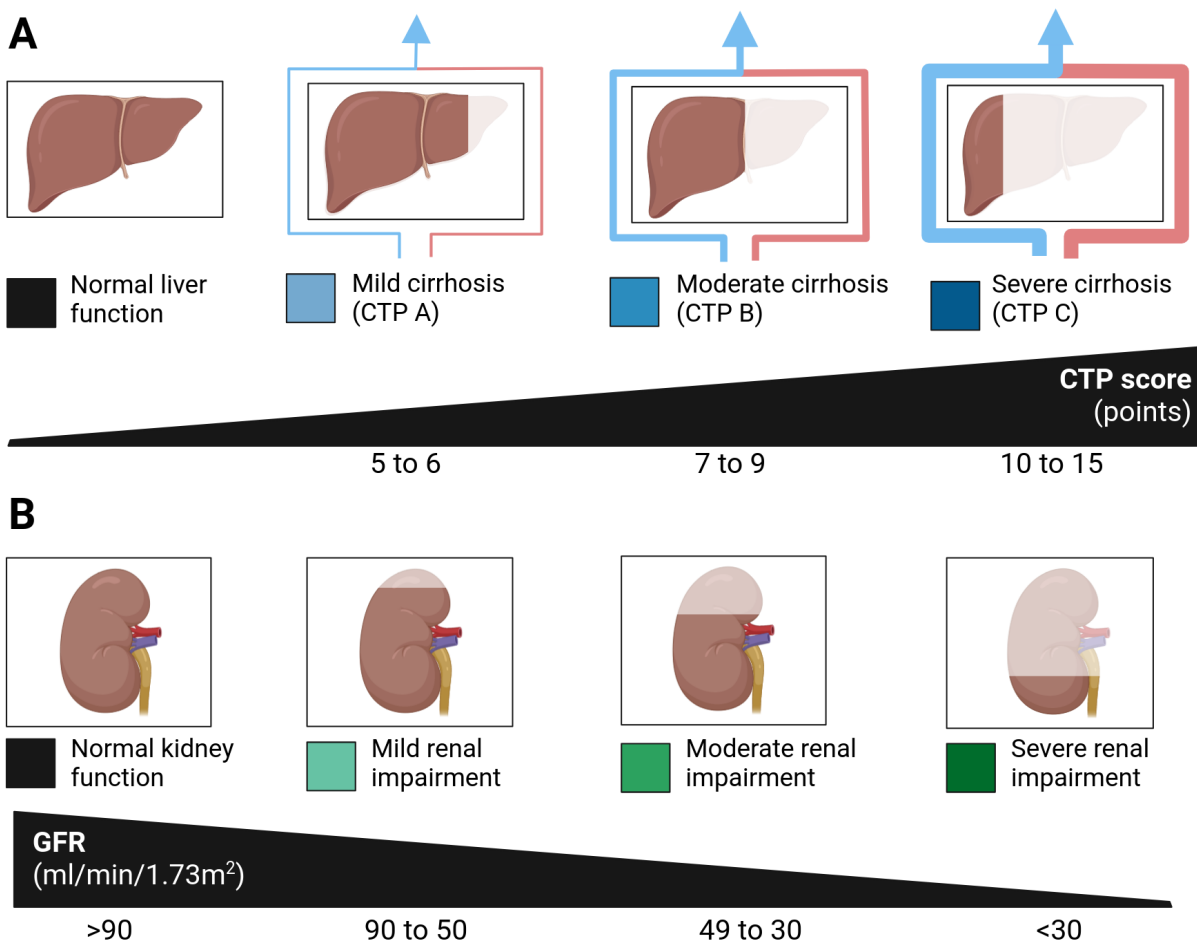


**Figure 3.5: Model of hepatic and renal impairment.** (A) The hepatic scans showing CTP score of 0 to 4 for normal liver function, 5 to 6 for mild cirrhosis (CTP A), 7 to 9 for moderate cirrhosis (CTP B), and 10 to 15 for severe cirrhosis (CTP C). (B) The renal scans showing GFR values greater than 90 (normal kidney function), 90 to 50 (mild renal impairment), 49 to 30 (moderate renal impairment) and less than 30 (severe renal impairment)

**Renal functional impairment:** Renal impairment (Fig. 3.5B) was defined using the parameter  $KI_{\text{f\_renal\_function}}$ , which varied from 0.1 to 1.9, and represents the change in the ability of the kidney to excrete sorafenib in the urine.

The values for mild, moderate, and severe renal impairment were calculated by dividing the creatinine clearance of each impairment group by the creatinine clearance in healthy subjects, as reported in the study by Aboualfa et al [1]. The parameter values used were 1.00 for the control group, 0.69 for mild renal impairment, 0.32 for moderate renal impairment, and 0.19 for severe renal impairment.

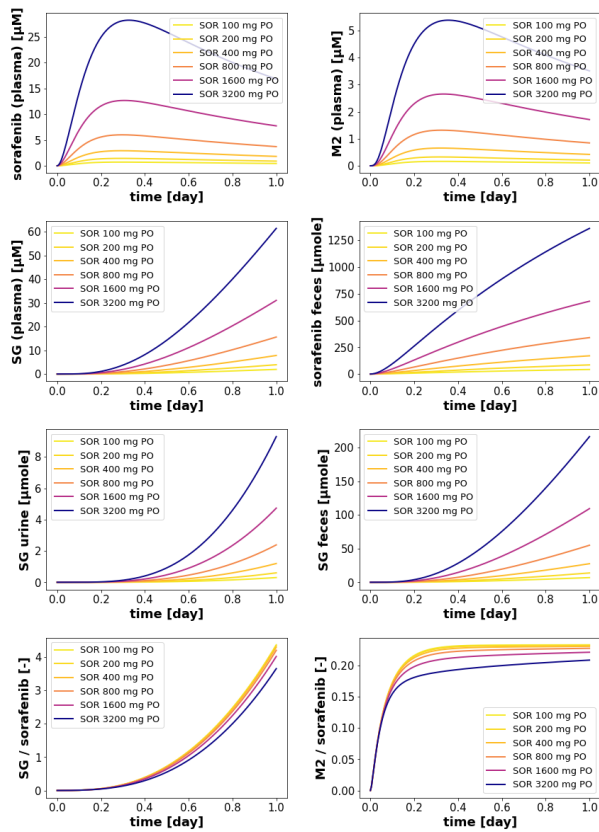
### 3.3 Model application

The developed PBPK model of sorafenib was applied to investigate the dose dependency of sorafenib PK and PK differences between healthy subjects and those with hepatic or renal impairment. Systematic scans were conducted on parameters to assess changes in sorafenib PKs in response to different degrees of renal and hepatic functional impairment.

#### 3.3.1 Dose dependency (single & multi dose)

The developed PBPK model can be applied to study the dose-dependency in pharmacokinetics after single or multiple oral sorafenib administration of varying doses of sorafenib (Fig. 3.6).

##### A. Oral sorafenib: Single dose



##### B. Oral sorafenib: Multi dose

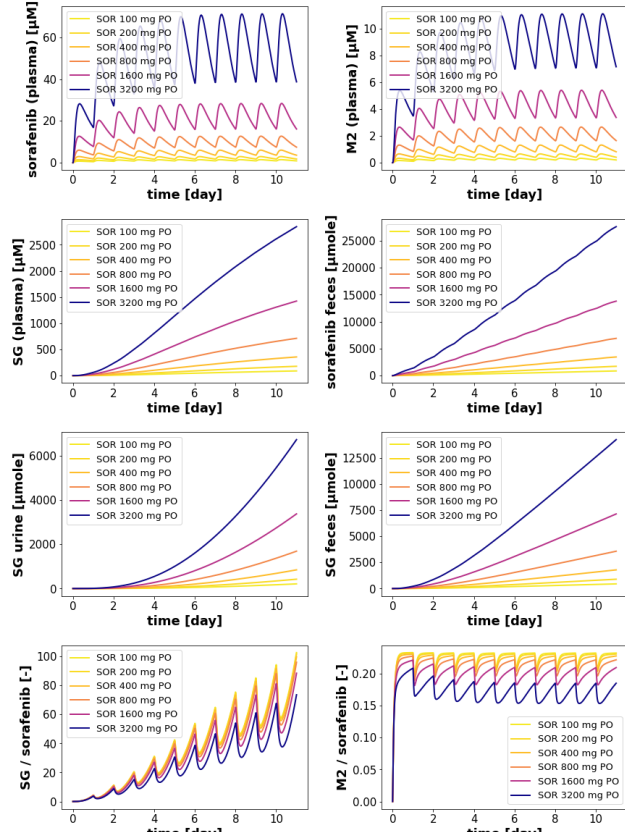


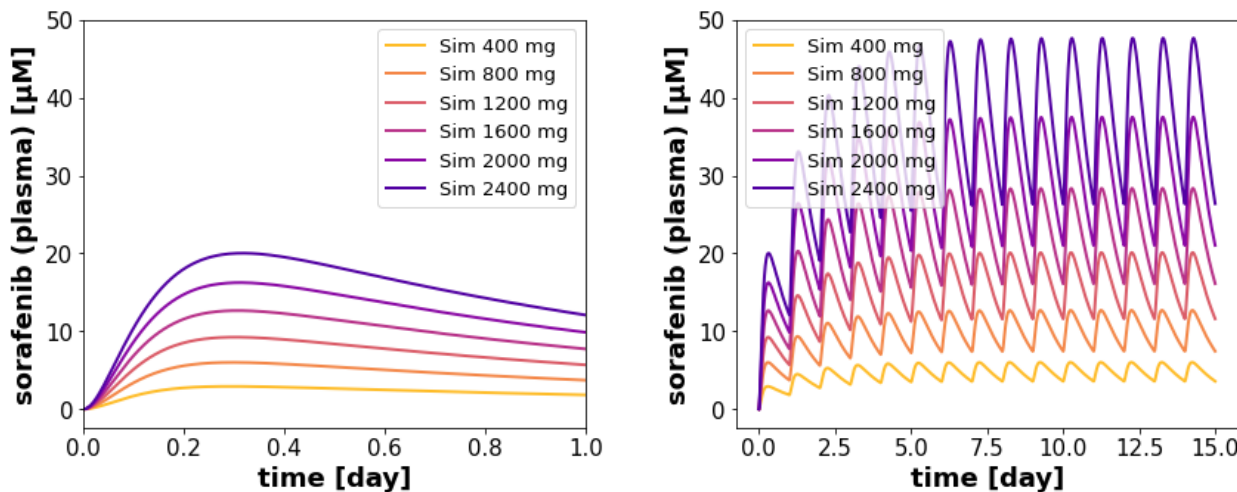
**Figure 3.6: Simulation of sorafenib's dose dependency.** Depicting single (A) and multiple (B) oral dose simulation with 100, 200, 400, 800, 1600, 3200 mg doses and corresponding concentration of sorafenib (SOR), sorafenib-N-oxide (M2), sorafenib-glucuronide (SG) in plasma, urine, faeces as well as the SG/SOR and M2/SOR metabolic ratios

The model predicts an increase in the concentration of sorafenib (SOR), sorafenib N-oxide (M2) and sorafenib glucuronide (SG) in plasma, urine and feces with increasing sorafenib dose after single oral dosing (Fig. 3.6A) and multiple oral dosing (Fig. 3.6B). Compared to the single oral dose, the multiple oral dose simulation showed a 2-fold increase in plasma SOR and M2. The metabolic M2/SOR and SG/SOR ratios decreased proportionally at high doses.

### 3.3.2 Dose-dependent pharmacokinetic parameters

From the plasma time courses of sorafenib the dose-dependent PK parameters were calculated. The higher doses (darker colors) result in correspondingly high sorafenib plasma concentrations. With increasing sorafenib dose, the AUC of sorafenib increases as does the tmax (Fig. 3.7B), in accordance with the observations of Hornecker et al. [24]. In addition, Cmax and kel of sorafenib also increase in a dose-dependent manner.

#### A. Oral sorafenib:single and multi dose



#### B. Dose-dependency PK parameters

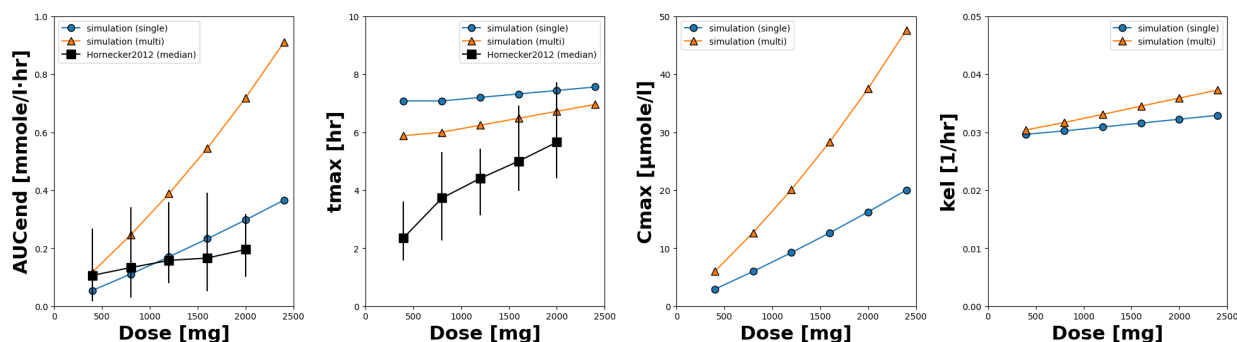


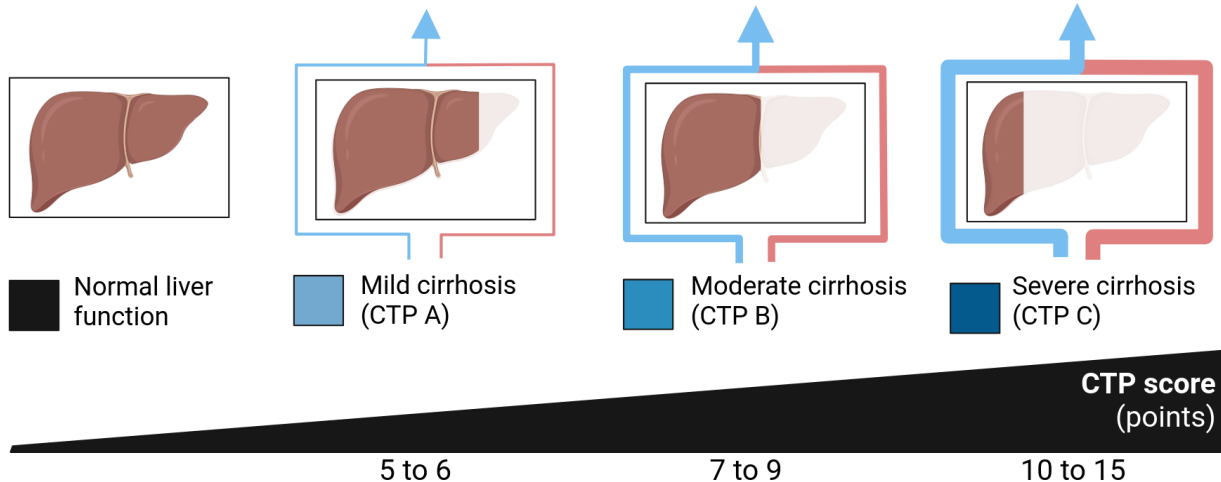
**Figure 3.7: Dose dependency of sorafenib PK parameters.: (A)** Sorafenib plasma pharmacokinetics after single and multiple oral doses (400, 800, 1200, 1600, 2000, 2400) of sorafenib. **(B)**. Sorafenib's pharmacokinetic parameters (AUC, tmax, Cmax and kel) for the first (single) and last dose (multi). For AUC and tmax data from Hornecker et al. is depicted [24].

The dose of sorafenib has a major effect on the PK of sorafenib with multiple dosing resulting in a dose accumulation compared to single dosing.

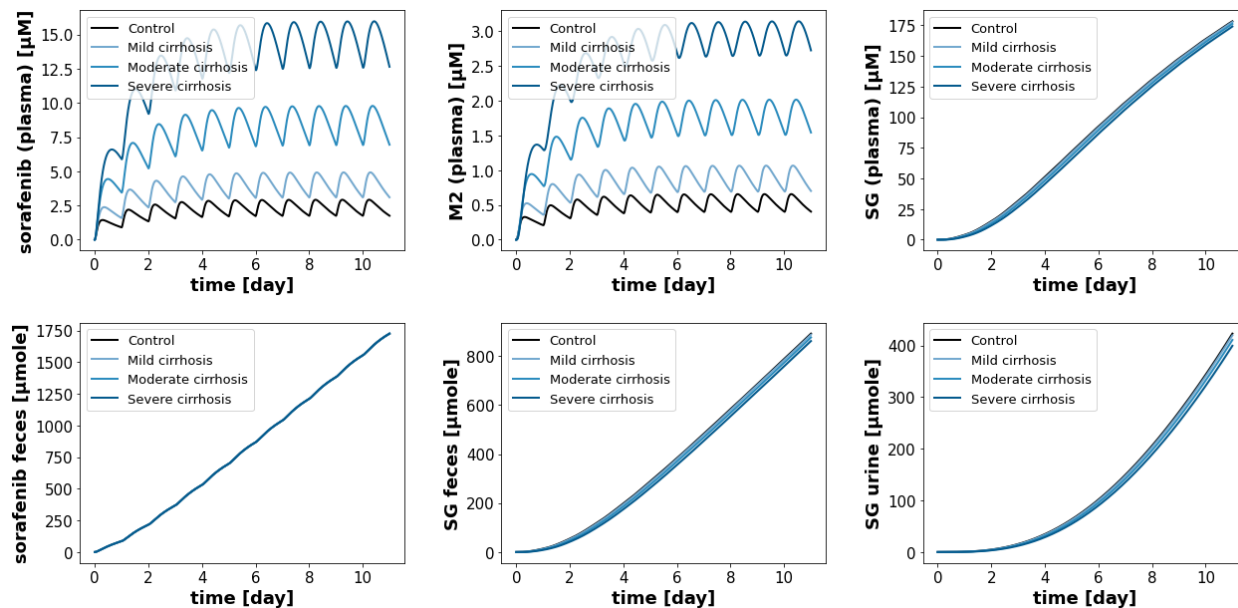
### 3.3.3 Hepatic impairment

Next the model was applied to study the effect of hepatic functional impairment on sorafenib PK (Fig. 3.8). Liver functional impairment significantly impacts the PK of sorafenib resulting in a strong increase in sorafenib and M2 plasma concentrations (Fig. 3.8B). SG on the other hand is not affected by hepatic impairment.

#### A. Degree of cirrhosis.



#### B. Sorafenib, M2 and SG concentration in cirrhosis.



### C. Hepatic impairment effect on sorafenib PK parameters

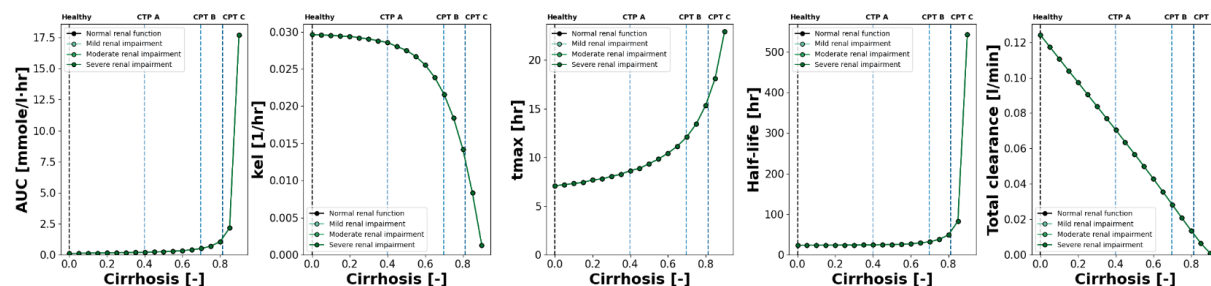


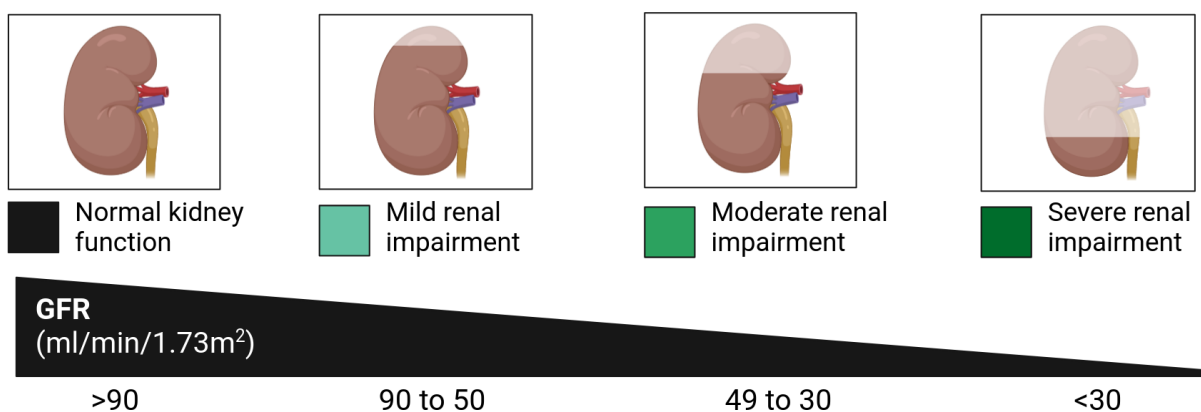
**Figure 3.8: The effect of hepatic impairment.** (A). Liver scans showing CPT for mild, moderate and severe hepatic impairment. (B). In hepatic impairment sorafenib (SOR), sorafenib-N-oxide (M2) and sorafenib glucuronide (SG) concentrations in plasma as well as SOR and SG concentrations in faces and SG concentrations in urine (C). Effect of hepatic impairment (cirrhosis) on sorafenib's PK parameters (AUC,  $k_{el}$ ,  $t_{max}$ ,  $t_{half}$  and total clearance) after a single dose of 400 mg sorafenib.

The plasma SOR, M2 increases with increasing severity of liver cirrhosis. For the sorafenib's PK parameters (Fig 3.8C), AUC (mmole/l·hr) increases with increasing severity of cirrhosis with estimated values for healthy (0.3), CTP-A (0.5), CTP-B (0.7) and CTP-C (1.0),  $k_{el}$  (1/hr) decreases with increasing cirrhosis for healthy (0), CTP-A (0.40), CTP-B (0.70) and CTP-C (0.81),  $t_{max}$  (hr) increases with increasing cirrhosis for healthy (7.5), CTP-A (8), CTP-B (12) and CTP-C (12),  $t_{half}$  (hr) increases with increasing cirrhosis for healthy (20), CTP-A (20), CTP-B (30) and CTP-C (50) as well as total Cl (l/min) decreases with degree of cirrhosis for healthy (0.12), CTP-A (0.07), CTP-B (0.02) and CTP-C (0.01). Accompanying renal impairment does not further alter the PK parameters of sorafenib.

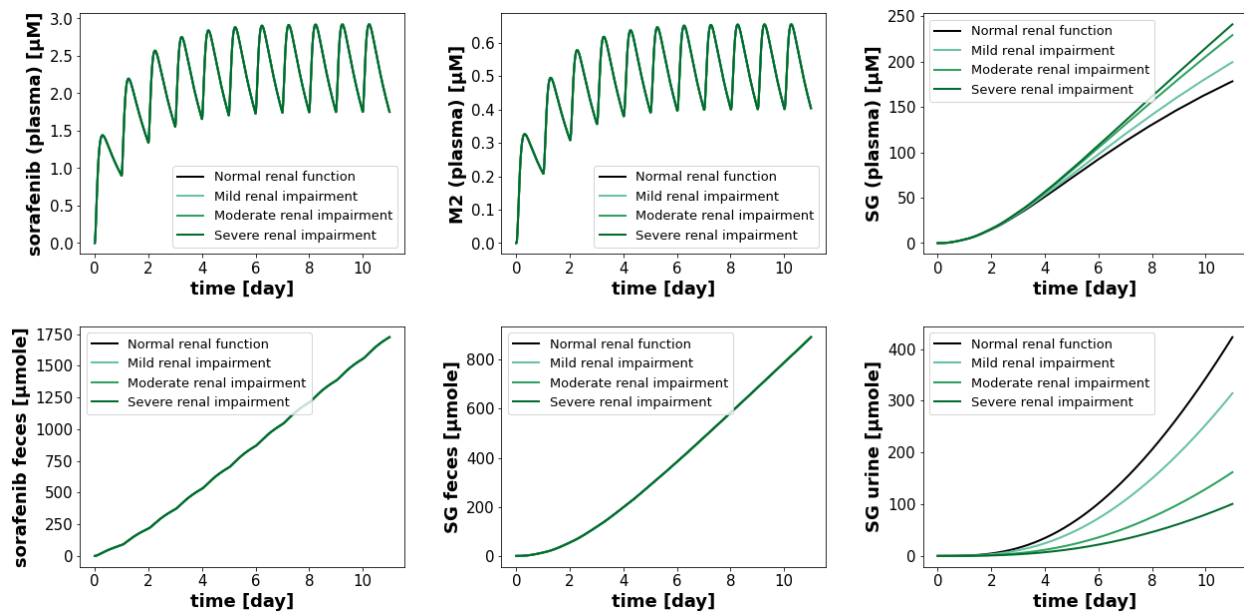
#### 3.3.4 Renal impairment

Next, the effect of renal functional impairment on the sorafenib PK was studied (Fig 3.9). In contrast to hepatic impairment sorafenib and M2 plasma concentrations are not affected by renal impairment, but SG plasma concentrations increase with increasing renal impairment. Renal functional impairment does not alter the PK parameters of sorafenib and M2 (Fig 3.9C), whereas hepatic functional impairment does strongly affect the PK of sorafenib. In contrast, hepatic functional impairment does not alter SG pharmacokinetics, but strongly affects SOR and M2.

##### A. Degree of renal impairment.



## B. SOR, M2 and SG concentrations in renal impairment.



## C. Renal impairment effect on sorafenib's PK parameter.

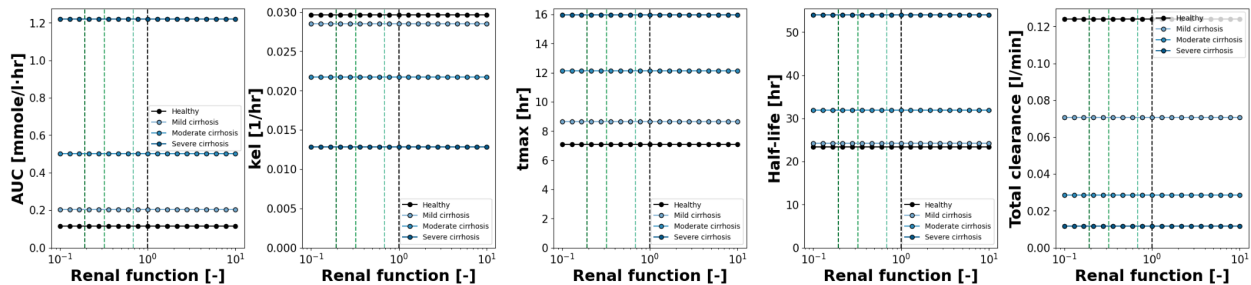


**Figure 3.9: The effect of renal impairment on PK parameters (A).** Kidney scans showing varying degrees of impairment with the GFR values for normal (>90), mild(50 - 90), moderate (30 - 49) and severe (>30) (B). In renal impairment sorafenib (SOR), sorafenib-N-oxide (M2) and sorafenib glucuronide (SG) concentrations in plasma as well as SOR and SG concentrations in faces and SG concentrations in urine. (C). Effect of renal impairment on sorafenib's PK parameter (AUC,  $k_{el}$ ,  $t_{max}$ ,  $t_{half}$  and total clearance after a single dose of 400 mg sorafenib.

## 3.4 Model performance

The model's performance was assessed by comparing model predictions to literature data. The resulting concentration-time plots show model predictions (solid lines) to curated literature data with legend in the upper right about title study and number of subjects (n) reported in study.

### 3.4.1 Single oral dose simulation

Model performance was evaluated for oral administration of sorafenib with a single dose in seven studies (Fig. 3.10 and Fig. 3.11). Data was overall in agreement with the simulations, but very large variability between the different studies was observed. The model application of single oral dose simulation with curated data from Hissaart2020 [27], Bins2017 [19] and Zimmerman2012 [31] studies with doses of 150, 200, 400, 600 and 800 mg showed a similar plasma concentration-time profile for SOR, M2 and SG in Fig. 3.10 while Huang2017 [25], Andriamanana2013 [17] and Hornecker2012 [24] studies in Fig. 3.11 showed slight discrepancies.

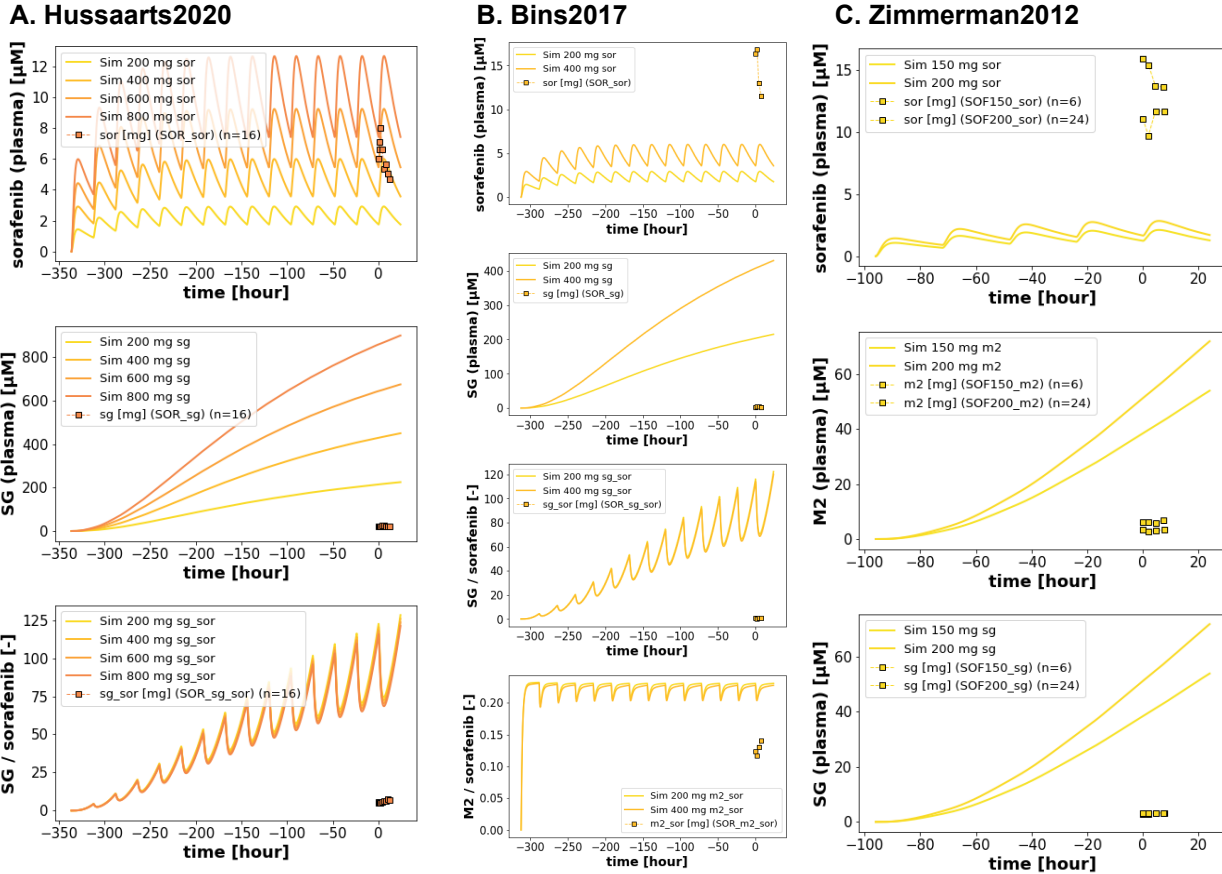


**Figure 3.10: Single oral dose simulation with curated data.** Plasma concentration time curve for sorafenib (SORr), sorafenib-N-oxide (M2) and sorafenib glucuronide (SG) with data from (A). Hussaart2020 [27], (B). Bins2017 [19] and (C). Zimmerman2012 [31] studies.

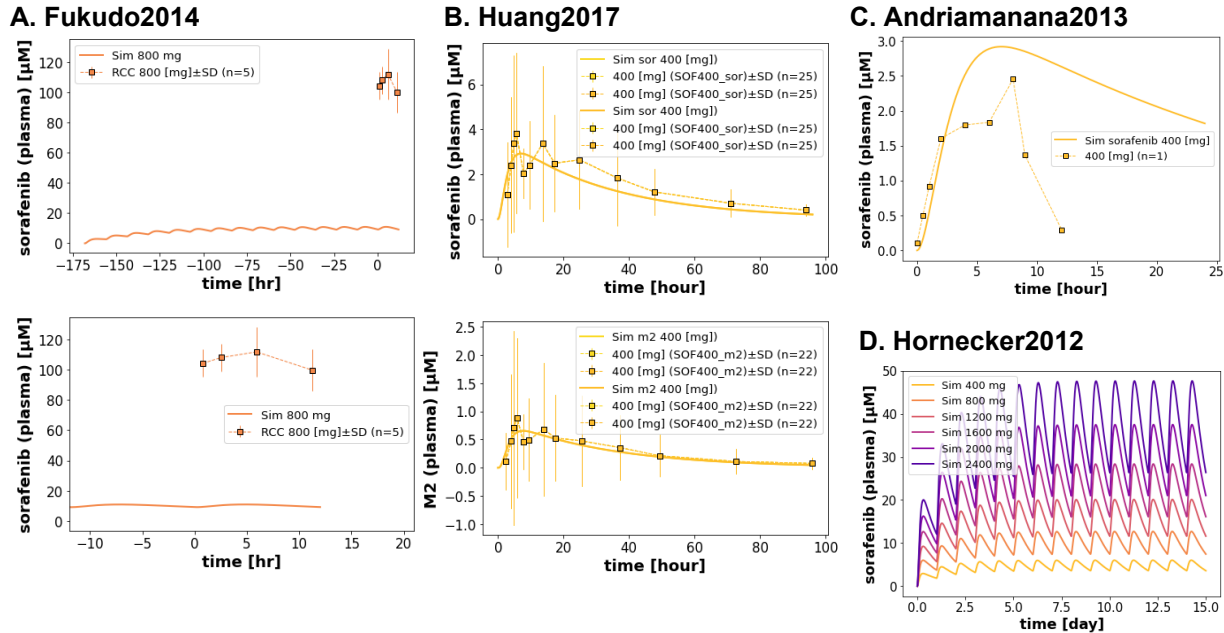


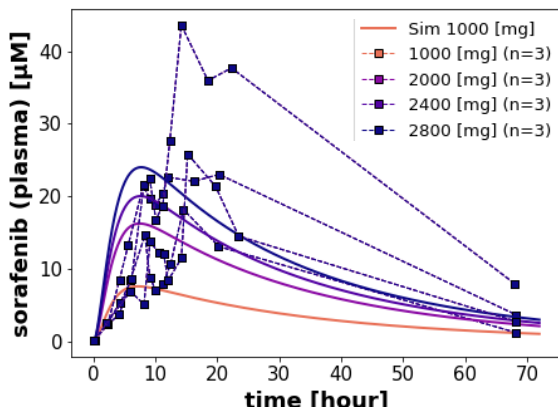
**Figure 3.11: Single oral dose simulation with curated data.** Plasma sorafenib concentration time curve simulated with data from (A). Fukudo2014 [23], (B). Huang2017 [25], (C). Andriamanana2013 [17] and (D). Hornecker 2012 [24] studies

### 3.4.2 Multiple oral dose simulation

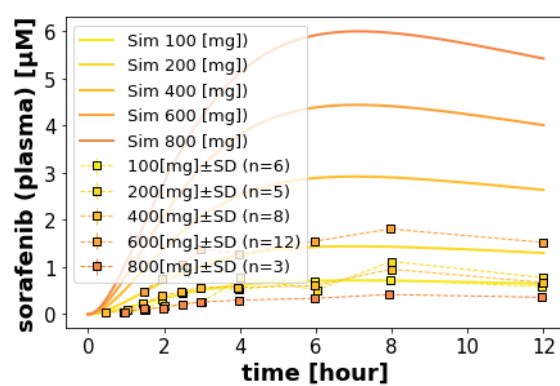
Model performance was evaluated for oral administration of sorafenib in five studies (Fig. 3.12 and Fig. 3.13) under multiple different doses.

Similarly to the single dose the multiple dose simulation with curated data from Mammatas2020 [29], Strumberg2005 [30], Duran2007 [20], Huh2021 [26] and Awada2005 [18] studies in Fig. 3.12 showed a similar plasma concentration-time profile for SOR, M2 and SG while Fucile2015 [22], and Ferrario2016 [21] studies in Fig. 3.13 showed discrepancies.

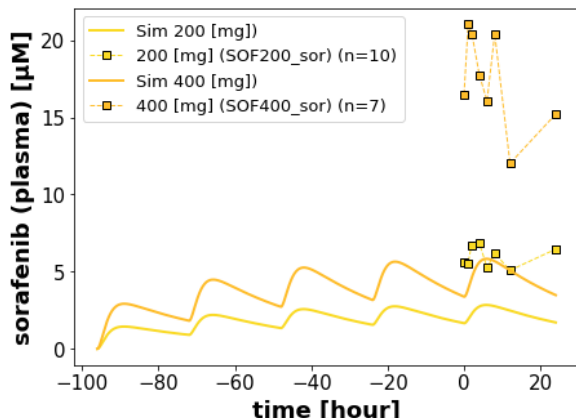
**A. Mammatas2020**



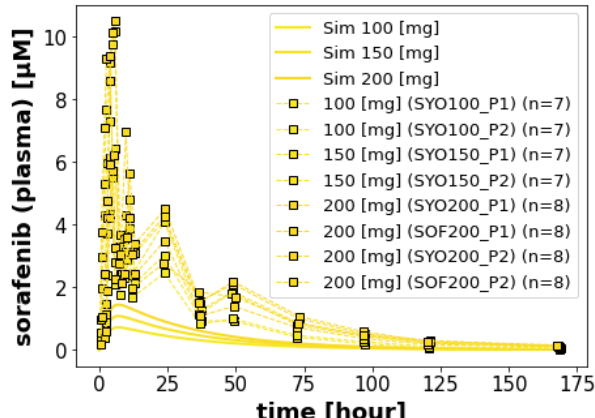
**B. Strumberg2005**



**C. Duran2007**



**D. Huh2021**



**E. Awada2005**

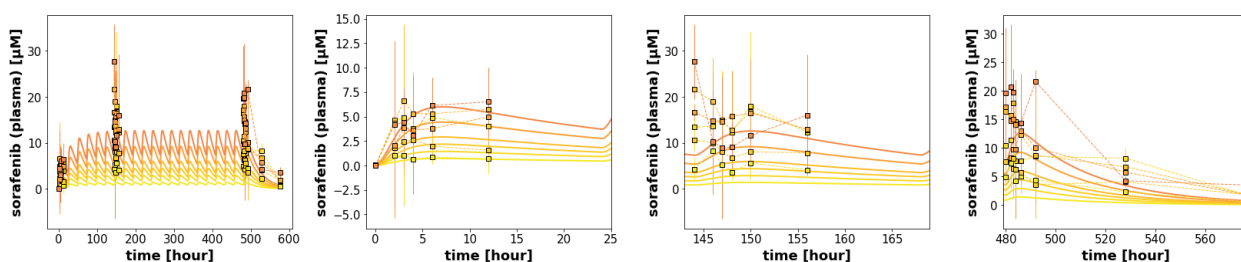


**Figure 3.12: Multiple oral dose simulation with curated data.** Plasma sorafenib concentration time curve simulated with data from (A). Mammatas2020 [29] (B). Strumberg2005 [30], (C).Duran2007 [20], (D).Huh2021 [26] and (E). Awada2005 [18] studies

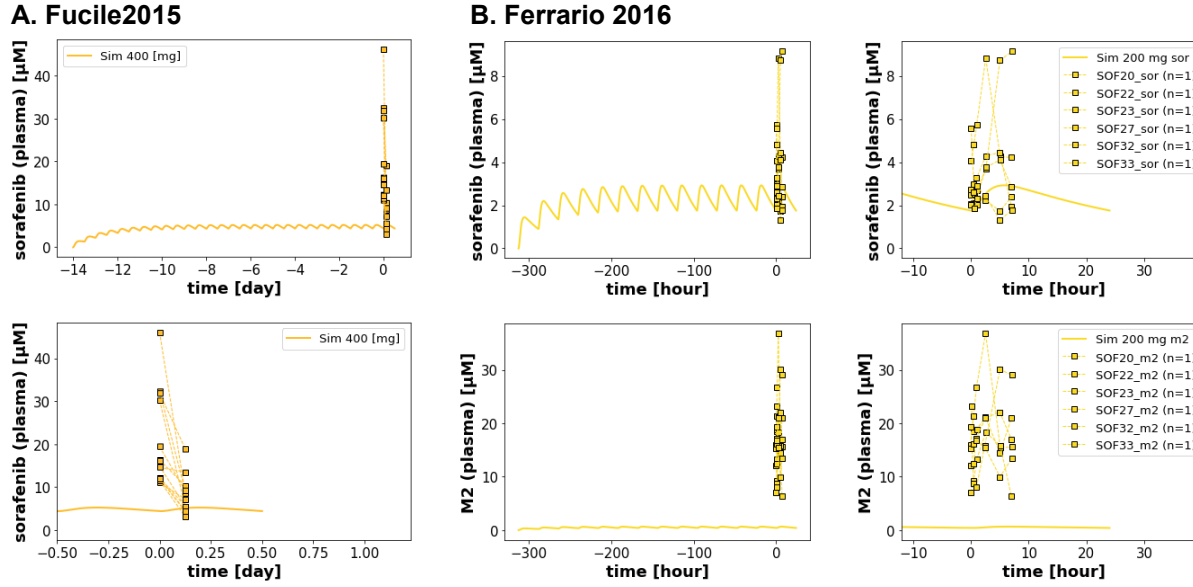


**Figure 3.13: Multiple oral dose simulation with curated data.** Plasma sorafenib concentration-time profile simulated with data from (A). Fucile2015 [22] and (B). Ferrario2016 [21] studies.

### 3.4.3 Hepatic and renal impairment

Hepatic functional impairment significantly impacts sorafenib PK resulting in elevated plasma concentrations. The more severe the hepatic impairment and cirrhosis, the higher the plasma concentrations.. In line with the model predictions, AbouAlfa2006 [14] showed an increase in plasma sorafenib concentrations with increasing degree of cirrhosis comparing HCC with CTP-A and CTP-B while sorafenib and M2 concentrations were not altered in renal functional impairment as expected in RCC when comparing simulations to data from Ishi2014 [24].

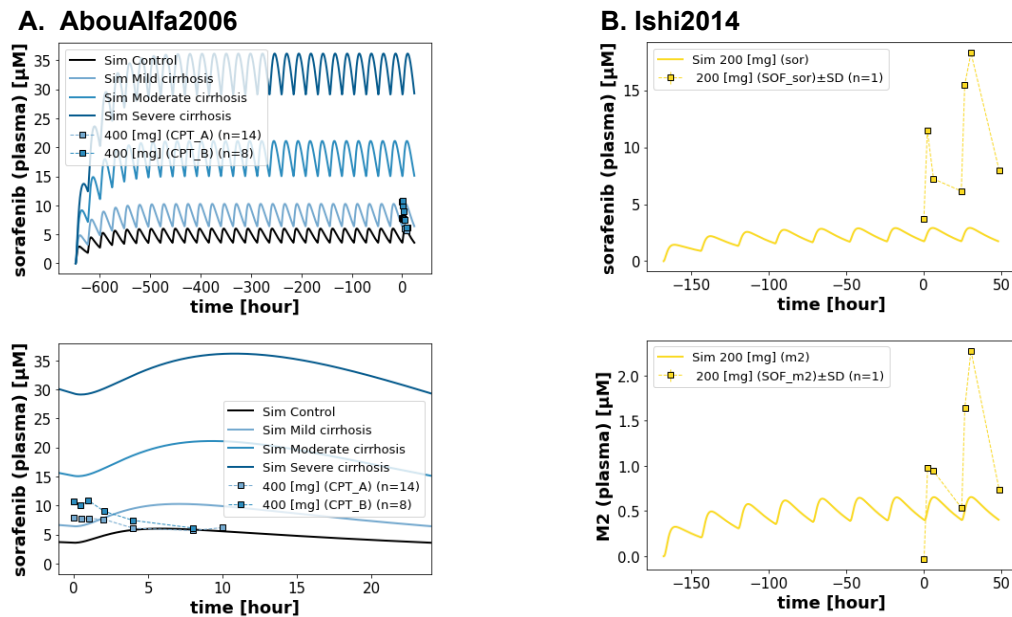


**Figure 3.14: Hepatic and renal impairment simulation with curated data.** (A). Simulation experiment for AbouAlfa2006 [16] with varying degrees of cirrhosis (CTP-A and CTP-B) in patients with HCC after 400 mg bid sorafenib for 28 days. (B). Ishi2014 [28] patients with kidney dysfunction in patients with RCC administered 200 mg sorafenib.

## 4 Discussion

In this work, a dataset of sorafenib (Tab. 1) was generated from 16 studies containing information on the time courses and pharmacokinetics following single and multiple oral administrations of sorafenib. The dataset was used to develop and validate a whole-body PBPK model (Fig. 3.4) of sorafenib consisting of organ submodels including intestine (Fig. 3.1), kidney (Fig. 3.2), liver (Fig. 3.3). The model allowed to simulate hepatic and renal functional impairment (Fig. 3.5). The PBPK model was used to investigate dose-response studies (Fig. 3.6), sorafenib PK parameters (Fig. 3.7) and its effect on hepatorenal impairment (Fig. 3.8). The model allows to predict the concentration-time profile of sorafenib (SOR), sorafenib N-oxide (M2) and sorafenib-glucuronide (SG) in plasma, urine and feces after single and multiple oral dosing as well as the effect of hepatorenal impairment on sorafenib PK parameters.

The model predictions for plasma, urine and fecal SOR, M2 and SG concentrations and PK parameters were consistent with the results of the selected sorafenib studies. In addition the model suggested a decreased liver uptake of sorafenib in liver with increasing cirrhosis which could lead to a prolonged drug residence time in the body and higher plasma levels.

The pharmacokinetics of sorafenib has been characterized by substantial variability and heterogeneity which could be attributed to factors such as age, comorbidities (particularly hepatic and renal impairment), lack of healthy control data, co-medication, the variability of the numerous metabolic enzymes and transporters involved and many studies which did change dosing throughout the study.

**Health Status:** An individual's health status plays a critical role for the pharmacokinetics of sorafenib. Patient age, the presence of comorbidities (including hepatic and renal impairment), and the overall health condition contribute significantly to the observed variability in sorafenib exposure. For example, elderly patients or those with impaired organ function may have altered drug metabolism, which requires careful consideration and potentially adjusted dosing strategies to optimize therapeutic outcomes.

**Heterogeneous data:** The lack of consistent and homogeneous data makes it difficult to understand the PK profile of sorafenib. Each study is characterized by highly heterogeneous cohorts, making it difficult to establish a unified model that accurately represents the drug's behavior. The lack of healthy control data for sorafenib is also challenging, as comparisons to a healthy baseline are essential to assess deviations caused by diseases or other factors. Without these healthy control data, recommendations for optimal dosing and treatment strategies become speculative, and the clinical implications of the observed variability remain unclear.

**Dosing regimes:** The dosing regime of sorafenib also contributes to the complexity of understanding its PK, as the variability in the amount administered and the frequency of administration between subjects in different studies adds to the challenge of establishing standardized dosing recommendations.

The variable dosing regimes observed in the literature highlight the importance of carefully adjusting doses based on individual patient characteristics and treatment goals.

**Co-medication:** Co-administration of sorafenib with other drugs significantly affects its PK profile because induction or inhibition of CYP3A4 and UGT1A9, two important enzymes involved in the metabolism of sorafenib, can significantly affect the efficacy and safety. Induction of these metabolic enzymes could increase its metabolism and decrease exposure whereas inhibition could increase exposure. Various co-medications contribute to the overall variability of sorafenib metabolism and exposure. The discussion of drug-drug interactions highlights the importance of considering specific pathways and enzymes involved in sorafenib metabolism. A comprehensive understanding of these drug-drug interactions is essential to predict the efficacy and potential adverse effects of sorafenib in different patient populations and to optimize therapeutic outcomes that minimize adverse effects associated with drug-drug interactions.

**Metabolic enzymes and transporters:** Differences in hepatic transporters, in addition to metabolizing enzymes, contribute to significant variability in the PK of sorafenib. Studies have shown that enzymes such as CYP3A4 and transporters such as OCT1, OATP1B1, OATP1B3, P-GP, and BCRP contribute to the uptake, efflux, and overall systemic exposure of sorafenib. Variations in these transporters, whether due to genetics or co-medication, may influence systemic exposure and response to sorafenib. Understanding these intricate pathways is essential for predicting inter-individual variability and implementing personalized treatment approaches.

**Toxicity:** The pharmacokinetic complexity of sorafenib includes toxicity issues. Given the difficulty in predicting individual responses to any drug, management of potential side effects is critical. The risk of adverse effects is influenced by factors such as exposure time, cumulative dosage, and individual patient characteristics. Understanding the relationship between pharmacokinetic parameters and toxicity is critical for modifying sorafenib therapy regimens to balance therapeutic benefit with the potential risk of harmful side effects.

## **5 Outlook**

The presented research is an important step forward to better understand the complex PK profile of sorafenib. The developed physiologically based pharmacokinetic (PBPK) model, based on systematic data integration and modeling, can serve as a tool to understand the behavior of sorafenib in the human body. However, it's important to note that this model, in its current form, has limitations due to the substantial heterogeneity and variability in clinical data it is based on. This underscores an important lesson: applying a universal, one-size-fits-all approach to drug modeling may not be sufficient to capture the nuances of individual patient responses, especially when facing highly heterogeneous patient cohorts and dosing protocols.

Future advances in the field must focus on more personalized methods. This means tailoring the model to individual patient characteristics, genetic profiles, and drug interactions. This personalized approach is critical to optimizing sorafenib therapy, particularly in the context of complex diseases such as hepatocellular carcinoma.

While the current model is a fundamental step, it invites further refinement. Subsequent versions could incorporate factors such as genetic variations in metabolic enzymes and transporters, the intricacies of drug-drug interactions, and the optimization of sorafenib dosing schedules. Such enhancements could improve the accuracy and relevance of the model, making it an even more powerful tool for predicting drug behavior in diverse patient populations.

## References

- [1] G. M. Keating and A. Santoro, “Sorafenib,” *Drugs*, vol. 69, no. 2, pp. 223–240, Jan. 2009, doi: 10.2165/00003495-200969020-00006.
- [2] L. Gong, M. M. Giacomini, C. Giacomini, M. L. Maitland, R. B. Altman, and T. E. Klein, “PharmGKB summary: sorafenib pathways,” *Pharmacogenet. Genomics*, vol. 27, no. 6, pp. 240–246, Jun. 2017, doi: 10.1097/FPC.0000000000000279.
- [3] J. Grzegorzewski *et al.*, “PK-DB: pharmacokinetics database for individualized and stratified computational modeling,” *Nucleic Acids Res.*, vol. 49, no. D1, pp. D1358–D1364, Jan. 2021, doi: 10.1093/nar/gkaa990.
- [4] M. Hucka *et al.*, “The Systems Biology Markup Language (SBML): Language Specification for Level 3 Version 2 Core Release 2,” *J. Integr. Bioinforma.*, vol. 16, no. 2, p. 20190021, Jun. 2019, doi: 10.1515/jib-2019-0021.
- [5] S. M. Keating *et al.*, “SBML Level 3: an extensible format for the exchange and reuse of biological models,” *Mol. Syst. Biol.*, vol. 16, no. 8, p. e9110, Aug. 2020, doi: 10.15252/msb.20199110.
- [6] “matthiaskoenig/sbmlutils: Python utilities for SBML.” Accessed: Dec. 19, 2023. [Online]. Available: <https://github.com/matthiaskoenig/sbmlutils>
- [7] M. König and N. Rodriguez, “matthiaskoenig/cy3sbml: cy3sbml-v0.3.0 - SBML for Cytoscape.” Zenodo, Sep. 19, 2019. doi: 10.5281/zenodo.3451319.
- [8] M. König, A. Dräger, and H.-G. Holzhütter, “CySBML: a Cytoscape plugin for SBML,” *Bioinformatics*, vol. 28, no. 18, pp. 2402–2403, Sep. 2012, doi: 10.1093/bioinformatics/bts432.
- [9] M. König, “sbmlsim: SBML simulation made easy.” Zenodo, Sep. 27, 2021. doi: 10.5281/zenodo.5531088.
- [10] E. T. Somogyi *et al.*, “libRoadRunner: a high performance SBML simulation and analysis library,” *Bioinformatics*, vol. 31, no. 20, pp. 3315–3321, Oct. 2015, doi: 10.1093/bioinformatics/btv363.
- [11] C. Welsh, J. Xu, L. Smith, M. König, K. Choi, and H. M. Sauro, “libRoadRunner 2.0: A High-Performance SBML Simulation and Analysis Library.” arXiv, Feb. 25, 2022. doi: 10.48550/arXiv.2203.01175.
- [12] A. Köller, J. Grzegorzewski, and M. König, “Physiologically Based Modeling of the Effect of Physiological and Anthropometric Variability on Indocyanine Green Based Liver Function Tests,” *Front. Physiol.*, vol. 12, 2021, Accessed: Dec. 19, 2023. [Online]. Available: <https://www.frontiersin.org/articles/10.3389/fphys.2021.757293>
- [13] A. Köller, J. Grzegorzewski, H.-M. Tautenhahn, and M. König, “Prediction of survival after partial hepatectomy using a physiologically based pharmacokinetic model of indocyanine green liver function test.” 2021. doi: 10.1101/2021.06.15.448411.
- [14] B. S. Mallol, J. Grzegorzewski, H.-M. Tautenhahn, and M. König, “Insights into Intestinal P-glycoprotein Function using Talinolol: A PBPK Modeling Approach,” Systems Biology, preprint, Nov. 2023. doi: 10.1101/2023.11.21.568168.
- [15] F. Okibedi and M. König, “Physiologically based pharmacokinetic (PBPK) model of sorafenib.” Zenodo, Dec. 26, 2023. doi: 10.5281/zenodo.10432866.
- [16] G. K. Abou-Alfa *et al.*, “Phase II study of sorafenib in patients with advanced hepatocellular carcinoma.,” *J. Clin. Oncol. Off. J. Am. Soc. Clin. Oncol.*, vol. 24, no. 26, pp. 4293–4300, Sep. 2006, doi: 10.1200/JCO.2005.01.3441.

- [17] I. Andriamanana, I. Gana, B. Duretz, and A. Hulin, “Simultaneous analysis of anticancer agents bortezomib, imatinib, nilotinib, dasatinib, erlotinib, lapatinib, sorafenib, sunitinib and vandetanib in human plasma using LC/MS/MS.,” *J. Chromatogr. B Analyt. Technol. Biomed. Life. Sci.*, vol. 926, pp. 83–91, May 2013, doi: 10.1016/j.jchromb.2013.01.037.
- [18] A. Awada *et al.*, “Phase I safety and pharmacokinetics of BAY 43-9006 administered for 21 days on/7 days off in patients with advanced, refractory solid tumours.,” *Br. J. Cancer*, vol. 92, no. 10, pp. 1855–1861, May 2005, doi: 10.1038/sj.bjc.6602584.
- [19] S. Bins *et al.*, “Influence of OATP1B1 Function on the Disposition of Sorafenib- $\beta$ -D-Glucuronide.,” *Clin. Transl. Sci.*, vol. 10, no. 4, pp. 271–279, Jul. 2017, doi: 10.1111/cts.12458.
- [20] I. Duran *et al.*, “Phase I targeted combination trial of sorafenib and erlotinib in patients with advanced solid tumors.,” *Clin. Cancer Res. Off. J. Am. Assoc. Cancer Res.*, vol. 13, no. 16, pp. 4849–4857, Aug. 2007, doi: 10.1158/1078-0432.CCR-07-0382.
- [21] C. Ferrario *et al.*, “Phase I/II Trial of Sorafenib in Combination with Vinorelbine as First-Line Chemotherapy for Metastatic Breast Cancer.,” *PloS One*, vol. 11, no. 12, p. e0167906, 2016, doi: 10.1371/journal.pone.0167906.
- [22] C. Fucile *et al.*, “Measurement of sorafenib plasma concentration by high-performance liquid chromatography in patients with advanced hepatocellular carcinoma: is it useful in clinical practice? A pilot study.,” *Med. Oncol. Northwood Lond. Engl.*, vol. 32, no. 1, p. 335, Jan. 2015, doi: 10.1007/s12032-014-0335-7.
- [23] M. Fukudo *et al.*, “Exposure-toxicity relationship of sorafenib in Japanese patients with renal cell carcinoma and hepatocellular carcinoma.,” *Clin. Pharmacokinet.*, vol. 53, no. 2, pp. 185–196, Feb. 2014, doi: 10.1007/s40262-013-0108-z.
- [24] M. Hornecker *et al.*, “Saturable absorption of sorafenib in patients with solid tumors: a population model.,” *Invest. New Drugs*, vol. 30, no. 5, pp. 1991–2000, Oct. 2012, doi: 10.1007/s10637-011-9760-z.
- [25] F. Huang *et al.*, “No Effect of Levothyroxine and Levothyroxine-Induced Subclinical Thyrotoxicosis on the Pharmacokinetics of Sorafenib in Healthy Male Subjects.,” *Thyroid Off. J. Am. Thyroid Assoc.*, vol. 27, no. 9, pp. 1118–1127, Sep. 2017, doi: 10.1089/thy.2017.0085.
- [26] K. Y. Huh *et al.*, “Population Pharmacokinetic Modelling and Simulation to Determine the Optimal Dose of Nanoparticulated Sorafenib to the Reference Sorafenib.,” *Pharmaceutics*, vol. 13, no. 5, Apr. 2021, doi: 10.3390/pharmaceutics13050629.
- [27] K. G. A. M. Hussaarts *et al.*, “Influence of Probenecid on the Pharmacokinetics and Pharmacodynamics of Sorafenib,” *Pharmaceutics*, vol. 12, no. 9, p. 788, Aug. 2020, doi: 10.3390/pharmaceutics12090788.
- [28] T. Ishii *et al.*, “Sorafenib in a hepatocellular carcinoma patient with end-stage renal failure: A pharmacokinetic study.,” *Hepatol. Res. Off. J. Jpn. Soc. Hepatol.*, vol. 44, no. 6, pp. 685–688, Jun. 2014, doi: 10.1111/hepr.12156.
- [29] L. H. Mammatas *et al.*, “Sorafenib administered using a high-dose, pulsatile regimen in patients with advanced solid malignancies: a phase I exposure escalation study.,” *Cancer Chemother. Pharmacol.*, vol. 85, no. 5, pp. 931–940, May 2020, doi: 10.1007/s00280-020-04065-5.
- [30] D. Strumberg *et al.*, “Phase I clinical and pharmacokinetic study of the Novel Raf kinase and vascular endothelial growth factor receptor inhibitor BAY 43-9006 in patients with

- advanced refractory solid tumors.,” *J. Clin. Oncol. Off. J. Am. Soc. Clin. Oncol.*, vol. 23, no. 5, pp. 965–972, Feb. 2005, doi: 10.1200/JCO.2005.06.124.
- [31] E. I. Zimmerman *et al.*, “Contribution of OATP1B1 and OATP1B3 to the disposition of sorafenib and sorafenib-glucuronide.,” *Clin. Cancer Res. Off. J. Am. Assoc. Cancer Res.*, vol. 19, no. 6, pp. 1458–1466, Mar. 2013, doi: 10.1158/1078-0432.CCR-12-3306.

## **Acknowledgements**

This work was supported by the Federal Ministry of Education and Research (BMBF, Germany) within ATLAS by grant number 031L0304B and by the German Research Foundation (DFG) within the Research Unit Program FOR 5151 “QuaLiPerF (Quantifying Liver Perfusion-Function Relationship in Complex Resection - A Systems Medicine Approach)” by grant number 436883643 and by grant number 465194077 (Priority Programme SPP 2311, Subproject SimLivA).